Mon. Not. R. Astron. Soc. **296,** 502–522 (1998)

Evolutionary sequences for Nova V1974 Cygni using new nuclear reaction rates and opacities

S. Starrfield,[1,⋆] J. W. Truran,[2,⋆] M. C. Wiescher[3,⋆] and W. M. Sparks[4,⋆]

[1]*Department of Physics and Astronomy, Arizona State University, PO Box 871504, Tempe, AZ 85287-1504, USA*
[2]*Department of Astronomy and Astrophysics and Enrico Fermi Institute, University of Chicago, Chicago, IL 60637, USA*
[3]*Department of Physics, University of Notre Dame, Notre Dame, IN 46556, USA*
[4]*XNH, Nuclear and Hydrodynamic Applications, MS F664, Los Alamos National Laboratory, Los Alamos, NM 87544, USA*

Accepted 1997 November 12. Received 1997 September 26; in original form 1997 January 24

ABSTRACT

The outburst of Nova V1974 Cyg 1992 is arguably the best observed of this century, with realistic estimates now available for the amount of mass ejected, the composition of the ejecta and the total energy budget. These data strongly support the conclusion that this was indeed a 'neon' nova that occurred on an oxygen, neon, magnesium white dwarf. In addition, X-ray studies of its outburst imply that the mass of the white dwarf is about 1.25 $M_{\odot}$. We, therefore, report on the results of new calculations of thermonuclear runaways on 1.25-$M_{\odot}$ oxygen, neon, magnesium white dwarfs, using our one-dimensional, fully implicit, hydrodynamic stellar evolution code that includes a large nuclear reaction network. We have updated the nuclear reaction network, with the inclusion of new and improved experimental and theoretical determinations of the nuclear reaction rates. We have also incorporated the OPAL carbon rich tables and have investigated the effects of changes in convective efficiency on the evolution. Our results show that the changes in the reaction rates and opacities that we have introduced produce important changes with respect to our previous studies. For example, relevant to nucleosynthesis considerations, a smaller amount of ^{26}Al is produced, while the abundances of ^{31}P and ^{32}S increase by factors of more than two. This change is attributed to the increased proton-capture reaction rates for some of the intermediate mass nuclei near ^{26}Al and beyond, such that nuclear fusion to higher mass nuclei is enhanced. The characteristics of our models are then compared to observations of the outburst of V1974 Cyg 1992 and we find that the predicted amount of mass ejected is at least a factor of 10 less than observed. The low values for the amount of ejected mass are a consequence of the fact that the OPAL opacities are larger than those we previously used, which results in less mass being accreted on to the white dwarf. This is a general problem with respect to the comparison of observations and theory for ONeMg novae and we suggest a possible resolution of this discrepancy.

Key words: convection – nuclear reactions, nucleosynthesis, abundances – stars: activity – stars: individual: Nova V1974 Cygni – novae, cataclysmic variables – white dwarfs.

1 INTRODUCTION

It is now commonly accepted that a classical nova outburst is caused by a thermonuclear runaway (hereafter, TNR) that occurs in the accreted hydrogen-rich envelope of a white dwarf (hereafter, WD) in a close binary system (Truran 1982, 1990; Starrfield 1989, 1993, 1995). The secondary star in this cataclysmic variable (CV) binary system fills its Roche lobe and loses mass through the inner Lagrangian point into the lobe surrounding the WD. The material enters the Roche lobe of the WD with the angular momentum of the secondary and, therefore, creates an accretion disc before falling on to the WD. Observational determinations of the elemental abundances in nova ejecta have shown that the abundances are very non-solar and strongly imply that, at some time during the evolution, material from the WD core is mixed into the gas accreted from the secondary (Truran 1990; Starrfield et al. 1996b, and references therein). Neither the mechanism responsible for the mixing nor the phase of the outburst in which the mixing occurs is universally accepted.

Hydrodynamic studies have shown that the consequences of this accretion is a growing layer of hydrogen-rich gas on the WD. When

⋆ E-mail: sumner.starrfield@asu.edu(SS);truran@nova.uchicago.edu (JWT); Michael.C.Wiescher.1@nd.edu(MCW); wms@lanl.gov(WMS)

both the WD luminosity and the rate of mass accretion on to the WD are sufficiently low, such that the deepest layers of the accreted material become electron degenerate, a TNR occurs near the base of the accreted layers. For the physical conditions of temperature and density that are expected in this environment, thermonuclear burning proceeds by means of hydrogen burning, first from the proton–proton chain and, subsequently, via the carbon, nitrogen and oxygen (CNO) cycles, through the peak of the outburst. If there are heavier nuclei present in the nuclear burning shell, they contribute significantly to the nucleosynthesis but, for the range of temperatures typically sampled in classical nova outbursts, they do not give rise to significant energy production. Both compressional heating and the energy released by the nuclear reactions heat the accreted material ($\sim 10^{-6}$ to $\sim 10^{-4}$ $M_{\odot}$, depending on WD mass) until an explosion occurs.

Energy production and nucleosynthesis associated with the CNO hydrogen burning reaction sequences impose interesting constraints on the energetics of the runaway: in particular, the rate of nuclear energy generation at high temperatures ($T > 10^8$ K) is limited by the time-scales of the *slower and temperature insensitive positron decays*, particularly ^{13}N ($\tau = 600$ s), ^{14}O ($\tau = 71$ s), ^{15}O ($\tau = 124$ s), and ^{18}F ($\tau = 109.8$ m). The behaviour of the positron decay nuclei holds important implications for the nature and consequences of classical nova outbursts. For example, significant enhancements of envelope CNO concentrations are required to insure higher levels of energy release on a hydrodynamic time-scale (seconds for WDs) and thus produce a violent outburst (Starrfield, Truran & Sparks 1978; Truran 1982; Starrfield 1995).

The large abundances of the positron decay nuclei, at the peak of the outburst, have important and exciting consequences for the evolution. (1) Since the energy production in the CNO cycle comes from proton captures, interspersed by β^+-decays, the rate at which energy is produced, at temperatures exceeding 10^8 K, depends only on the half-lives of the positron decay nuclei and the numbers of CNO nuclei initially present in the envelope. (2) Because convection operates throughout the entire accreted envelope, it brings unburned CNONeMg nuclei into the shell source, when the temperature is rising very rapidly, and keeps the nuclear reactions operating far from equilibrium. (3) Since the convective turn-over time-scale is $\sim 10^2$ s near the peak of the TNR, a significant fraction of the positron decay nuclei are able to reach the surface without decaying and the rate of energy generation at the surface can exceed 10^{13} to 10^{15} erg g^{-1} s^{-1} (depending upon the enrichment). (4) Because these nuclei decay when the temperatures in the envelope have declined to values that are too low for any further proton captures to occur, the isotopic ratios in the ejected material are distinctly different from those ratios predicted from studies of equilibrium CNONeMg burning. (5) Finally, since the decays of these nuclei provide an intense heat source throughout the envelope during the early phases of the explosion, they help eject the material from off the WD. Theoretical studies of this mechanism show that sufficient energy is produced, during the evolution described above, to eject material with expansion velocities that are in the range of the observed values and that the predicted bolometric light curves for the early stages are in reasonable agreement with the observations (Truran 1982; Starrfield 1989, 1995; Starrfield et al. 1992a; Politano et al. 1995).

An important development in studies of the nova outburst, has been the discovery of the oxygen, neon, magnesium (hereafter, ONeMg) compositional class of outburst (Williams et al. 1985; Starrfield, Sparks & Truran 1986). Our recent studies have shown that it is the outbursts that occur on ONeMg WDs that produce the most interesting nucleosynthesis (Weiss & Truran 1990; Nofar, Shaviv & Starrfield 1991; Starrfield et al. 1992a; Politano et al. 1995). The best studied ONeMg outburst was that of Nova V1974 Cyg in 1992. Detailed studies of its outburst have provided a wealth of new data on ONeMg nova outbursts and we concentrate on that class of novae in this paper.

In order to demonstrate that such outbursts exist, in Section 2 we briefly describe the abundance determinations for the ejecta of novae and provide an updated table of abundances determined from nebular techniques. In Section 3, we describe our hydrodynamic code and the recent changes that have been made to this code. We then, in Section 4, describe our new simulations; in Section 5, discuss the nucleosynthesis in one sequence; and in Section 6, compare these simulations to the observations of V1974 Cyg. We find a good deal of agreement in the gross features, except for the amount of mass ejected, which is too low in the simulations to agree with the observations. In Section 7, therefore, we propose a possible solution to this discrepancy. A summary and discussion follow in Section 8.

2 OXYGEN–NEON–MAGNESIUM NOVAE

2.1 V693 CrA 1981 and QU Vul 1984 No. 2

As we have shown in earlier papers, the production of large amounts of ^{22}Na, ^{26}Al and other intermediate mass nuclei in a nova outburst requires that the outburst occur on an ONeMg WD (Weiss & Truran 1990; Nofar, Shaviv & Starrfield 1991). Although Law & Ritter (1983) first suggested that such WDs might exist, it was the outburst of V693 CrA 1981 that confirmed that they did exist in nova systems (Williams et al. 1985). Ultraviolet spectroscopic data were obtained for this nova with the *International Ultraviolet Explorer* satellite (*IUE*) over a six-month period. It was clear from the last set of spectra obtained in 1981 September (which simultaneously showed strong [Ne IV] 1602 Å and 2420 Å) that neon was enriched in the ejecta. This was later confirmed by detailed analyses (Vanlandingham, Starrfield & Shore 1997, and references therein). Their results are given in Table 1, together with those for all other well-studied novae. This table represents a substantially updated version of that of Truran (1990; see also Livio & Truran 1994).

Given these data, Starrfield et al. (1986) performed a theoretical study of accretion on to massive WDs in which it was assumed that only the oxygen abundance was enhanced (their nuclear reaction network, at that time, did not include nuclei above fluorine), and showed that such an outburst would appear different from a nova with both carbon and oxygen enhanced (one that occurred on a CO WD). This is because the ^{12}C(p,γ)^{13}N reaction rate is substantially faster at lower temperatures than the ^{16}O(p,γ)^{17}F rate, so that the TNR occurs with less accreted material on the CO WD.

At virtually the same time that these exploratory calculations were in progress, Gehrz, Grasdalen & Hackwell (1985) reported that QU Vul 1984 No. 2 showed enhanced neon. These results, in combination with the *IUE* spectra that also showed strong neon lines (Starrfield 1988), implied that the ejecta of QU Vul were enriched in neon and magnesium, as was again confirmed by detailed analyses (Saizar et al. 1992; Andreä, Drechsel & Starrfield 1994; Austin et al. 1996). Truran & Livio (1986; see also Ritter et al. 1991 and Livio & Truran 1994) estimated that about one-third of all observed outbursts should be ONeMg novae.

2.2 V838 Her 1991 and V1974 Cyg 1992

Two recent outbursts have proven to be very important. Although

Table 1. Heavy-element mass fractions in novae from optical spectroscopy.

Object	Year	H	He	C	N	O	Ne	Na-Fe	Z	$Z/Z_\odot$	$Ne/Ne_\odot$	CNO/Ne-Fe
T Aur[4]	1891	0.47	0.40		0.079	0.051			0.13	6.8		
RR Pic[13]	1925	0.53	0.43	0.0039	0.022	0.0058	0.011		0.043	2.3	6.3	2.9
DQ Her[15]	1934	0.34	0.095	0.045	0.23	0.29			0.57	30.		
DQ Her[7]	1934	0.27	0.16	0.058	0.29	0.22			0.57	30.		
HR Del[12]	1967	0.45	0.48		0.027	0.047	0.0030		0.077	4.1	1.7	25.
V1500 Cyg[3]	1975	0.49	0.21	0.070	0.075	0.13	0.023		0.30	16.	13.	12.
V1500 Cyg[6]	1975	0.57	0.27	0.058	0.041	0.050	0.0099		0.16	8.4	5.6	15.
V1668 Cyg[11]	1978	0.45	0.23	0.047	0.14	0.13	0.0068		0.32	17.	3.9	47.
V1668 Cyg[1]	1978	0.45	0.22	0.070	0.14	0.12			0.33	17.		
V693 CrA[19]	1981	0.40	0.21	0.004	0.069	0.067	0.23	0.02	0.39	19.5	115.	0.56
V693 CrA[14]	1981	0.29	0.32	0.046	0.080	0.12	0.17	0.016	0.39	21.	97.	1.3
V693 CrA[1]	1981	0.16	0.18	0.0078	0.14	0.21	0.26	0.030	0.66	35.	148.	1.2
V1370 Aql[10]	1982	0.053	0.088	0.035	0.14	0.051	0.52	0.11	0.86	45.	296.	0.36
V1370 Aql[1]	1982	0.044	0.10	0.050	0.19	0.037	0.56	0.017	0.86	45.	296.	0.48
GQ Mus[5]	1983	0.37	0.39	0.0081	0.13	0.095	0.0023	0.0039	0.24	13.	1.2	38.
PW Vul[8]	1984	0.69	0.25	0.0033	0.049	0.014	0.00066		0.067	3.5	0.38	100.
PW Vul[1]	1984	0.47	0.23	0.073	0.14	0.083	0.0040	0.0048	0.30	16.	2.3	34.
QU Vul[9]	1984	0.30	0.60	0.0013	0.018	0.039	0.040	0.0049	0.10	5.3	23.	1.3
QU Vul[1]	1984	0.33	0.26	0.0095	0.074	0.17	0.086	0.063	0.40	21.	49.	1.7
QU Vul[2]	1984	0.36	0.19		0.071	0.19	0.18	0.0014	0.44	23.	100.	1.4
V842 Cen[1]	1986	0.41	0.23	0.12	0.21	0.030	0.00090	0.0038	0.36	19.	0.51	77.
V827 Her[1]	1987	0.36	0.29	0.087	0.24	0.016	0.00066	0.0021	0.35	18.	0.38	124.
QV Vul[1]	1987	0.68	0.27		0.010	0.041	0.00099	0.00096	0.053	2.8	0.56	26.
V2214 Oph[1]	1988	0.34	0.26		0.31	0.060	0.017	0.015	0.40	21.	9.7	12.
V977 Sco[1]	1989	0.51	0.39		0.042	0.030	0.026	0.0027	0.10	5.3	15.	2.5
V433 Sct[1]	1989	0.49	0.45		0.053	0.0070	0.00014	0.0017	0.062	3.3	0.80	33.
V351 Pup[16]	1991	0.37	0.25	0.0056	0.064	0.19	0.11		0.38	20.	63.	2.4
V1974 Cyg[2]	1992	0.19	0.32		0.085	0.29	0.11	0.0051	0.49	27.	68.	3.2
V1974 Cyg[17]	1992	0.30	0.52	0.016	0.023	0.102	0.037	0.075	0.18	9.7	21.	3.1
V838 Her[18]	1991	0.80	0.093	0.018	0.019	0.0032	0.068	0.0030	0.11	5.7	39.	0.56
Solar[20]		0.705	0.275	0.003	0.001	0.010	0.002	0.004	0.020	1.0	1.0	2.33

References. 1: Andrea et al. 1994; 2: Austin et al. 1995; 3: Ferland & Shields 1978; 4: Gallagher et al. 1980; 5: Morisset & Péquignot 1996; 6: Lance et al. 1988; 7: Petitjean et al. 1990; 8: Saizar et al. 1991; 9: Saizar et al. 1992; 10: Snijders et al. 1987; 11: Stickland et al. 1981; 12: Tylenda 1978; 13: Williams & Gallagher 1979; 14: Williams et al. 1985; 15: Williams et al. 1978; 16: Saizar et al. 1996; 17: Hayward et al. 1996; 18: Vanlandingham et al. 1996; 19: Vanlandingham et al. 1997; 20: Anders & Grevesse 1989.

there was strong circumstantial evidence that V838 Her 1991 was an ONeMg nova (Starrfield et al. 1993), confirmation came from analyses by Matheson, Filippenko & Ho (1993) and Vanlandingham et al. (1996), who reported that both neon and sulphur were enriched in the ejecta. The abundance determination for V838 Her (see Table 1) is in reasonable agreement with results of TNRs on massive ONeMg WDs (Starrfield et al. 1992a; Politano et al. 1995).

V1974 Cyg 1992 was the brightest nova seen in outburst since V1500 Cyg 1975 and it was observed from γ-ray to radio wavelengths. Important data were obtained by *ROSAT*, which was able to follow it through its entire X-ray outburst (Krautter et al. 1996) and *IUE* (Hauschildt et al. 1994a; Shore et al. 1993, 1994, 1996; Austin et al. 1996). In addition, its outburst was analysed with two new methods. First, Hauschildt et al. (1992, 1994a, 1994b, 1995, 1996) studied the early fireball stage with a non-LTE, spherical, expanding, model atmosphere code that was developed to study novae and supernovae. Secondly, Austin et al. (1996) developed a Metropolis et al. (1953; see also Press et al. 1992) simulated annealing algorithm to analyse nova nebular spectra and applied this method to V1974 Cyg. The abundance analysis of Austin et al. can be found in Table 1 and it showed that the enrichments were consistent with the outburst occurring on an ONeMg WD. Finally, both Shore et al. (1993) and Austin et al. (1996) obtained values for the ejected mass of $\sim 5 \times 10^{-5} M_\odot$. Because more data exists for the outburst of V1974 Cyg than for V838 Her, in this paper we will concentrate on V1974 Cyg.

Table 1 reveals that novae ejecta are enriched in the intermediate-mass elements. The mean heavy-element mass fraction for these *well-studied* cases is $Z = 0.34$ (we averaged multiple determinations for the same nova). The need to understand the cause of the large discrepancies between some of the abundance determinations, *for the same nova outburst*, warrants further study (Schwarz et al. 1997a,b; Vanlandingham et al. 1997). We also note that for at least three recent novae, V1370 Aql 1982, V2214 Oph 1988 and V838 Her 1991 the ejected material was enriched in sulphur as well as in neon and magnesium (Matheson et al. 1993; Andreä et al. 1994; Vanlandingham et al. 1996). The source of these large abundance enrichments must be matter dredged up from the underlying ONeMg WD and processed through hot, hydrogen burning. The production of sulphur requires, in addition, that the WD be massive (Starrfield et al. 1992a; Politano et al. 1995; Wanajoh, Nomoto, & Truran 1997). This implies that there likely are mass differences between the WDs in novae such as V838 Her 1991 and those in novae such as V1974 Cyg 1992 and V351 Pup 1991 (Starrfield et al. 1992a; Politano et al. 1995; Saizar et al. 1996).

Another important result was the fact that the *ROSAT* observations of Krautter et al. (1996) provided, for the first time, the complete X-ray light curve of a nova in outburst. Their data showed

that this nova was luminous in X-rays for about 18 months and that the constant bolometric luminosity phase lasted for about 14 months before the nova began a rapid decline. Krautter et al. were also able to show that the luminosity evolution and decline time-scale implied a mass for the WD of about $1.25\,M_\odot$ and, in addition, that $< 10^{-5}\,M_\odot$ of mixed (accreted plus core) material was left on the WD as a surface layer. Such a remnant layer should have converted most of its hydrogen to helium by the end of nuclear burning (Sparks et al. 1988; Fujimoto & Iben 1992). This result, in combination with arguments about the energetics of the outburst, was taken to imply that much of the helium found in the ejected gas came from the previous outburst in this system. We will return to this last result when we discuss the discrepancy between the amount of ejected gas that is observed and the amount predicted.

We have, earlier, studied accretion of hydrogen-rich material on to WDs with masses of 1.0, 1.25 and $1.35\,M_\odot$ (Politano et al. 1995). The analysis of the X-ray light curve of V1974 Cyg suggests that the mass of the WD in this system is $\sim 1.25\,M_\odot$ (Krautter et al. 1996). Within the context of stellar evolution, it is expected that the masses of ONeMg WDs should be greater than $\sim 1.2\,M_\odot$. For masses in this range, the TNR is usually found to occur prior to the accretion of $\sim 10^{-4}\,M_\odot$. Our previous studies of TNRs on 1.25-$M_\odot$ ONeMg WDs neither accreted nor ejected sufficient material to agree with the mass determinations for V1974 Cyg (Politano et al. 1995; Austin et al. 1996). We have, therefore, chosen to consider in this paper only 1.25-$M_\odot$ ONeMg WDs and to seek to identify the physical conditions that will yield larger accreted and ejected masses.

3 THE HYDRODYNAMIC CODE

In order to simulate the outbursts of ONeMg novae, we use the Lagrangian, one-dimensional, hydrodynamic computer code NOVA, which incorporates a large nuclear reaction network (see Politano et al. 1995, and references therein). The reaction network used in this study includes 78 nuclei ranging from hydrogen to calcium and is identical to that used in Politano et al. (1995; see also Weiss & Truran 1990). The nuclear reaction rates, however, have been updated to include those reported in Van Wormer et al. (1994) and Herndl et al. (1995). One of the purposes of this paper is to report how the introduction of new rates into the network has affected both the energy generation rate and the nucleosynthesis of nuclei in the range from oxygen to sulphur.

The new rates for proton capture reactions on short-lived, neutron deficient isotopes are based on the level structures of the respective compound nuclei (Van Wormer et al. 1994) and shell model predictions of the various decay channels of the resonance levels (Herndl et al. 1995). These rates differ considerably from previous estimates based on Hauser–Feshbach calculations. This can lead to significant changes in the reaction path, in particular for nova models with higher peak temperature conditions.

For many of the proton capture processes on stable and long-lived nuclei in the mass range A=20–40, extensive studies have been performed over the last few years to determine the reaction rates. These experimental results often have considerably changed the rates, in particular the results for ^{22}Na(p,γ) (Seuthe et al. 1990; Schmidt et al. 1995; Stegmüller et al. 1996), ^{23}Na(p,γ)(p,α) (Görres, Weischer & Rolfs 1989), ^{25}Mg(p,γ) (Iliadis et al. 1990,1996) and ^{27}Al(p,α) (Timmermann et al. 1989) may have significant influence on the predicted production of the long-lived γ-emitters ^{22}Na and ^{26}Al in novae. New experimental results concerning the reaction rates of ^{28}Si(p,γ) (Graff et al. 1990), ^{31}P(p,γ) (Iliadis et al. 1991), ^{31}P(p,α) (Iliadis et al. 1993; Ross et al 1995), ^{32}S(p,γ) (Iliadis et al. 1992b), ^{35}Cl(p,γ)(p,α) (Iliadis et al. 1994; Ross et al. 1995), and ^{36}Ar(p,γ) (Iliadis et al. 1992a) may significantly change the nucleosynthesis in the mass range above A=28 and influence the production of sulphur and argon which are both observed in the ejecta of ONeMg novae. In particular, it should be noted that the reaction rate for ^{32}S(p,γ) (Iliadis et al. 1992a) is considerably slower than previously anticipated (Woosley et al. 1975; Wallace & Woosley 1981) because of a level gap above the proton threshold. On the other hand the reaction ^{36}Ar(p,γ) (Iliadis et al. 1992a) is considerably faster than previously estimated (Wallace & Woosley 1981) because of additional low-energy resonances. All these changes to the reaction rates have been incorporated into our large nuclear reaction network and we will discuss the effects of these changes in Section 4.2.

In addition to the proton capture reactions, which are important for TNRs in novae, our network also includes the triple-alpha reaction, heavy-ion reactions(^{12}C + ^{12}C, ^{12}C + ^{16}O, ^{16}O + ^{16}O), all reactions involving neutrons, alpha particles, and photons, and all relevant weak interactions. The upper extent of this network is ^{40}Ca. For peak burning temperatures up to 4×10^8 K and dynamical time-scales characteristic of TNRs on massive WDs, this network provides a satisfactory treatment of nuclear energy generation and nucleosynthesis (Weiss & Truran 1990; Politano et al. 1995).

The second major change is that we now use the OPAL carbon-rich opacity tables for both the core and the accreted layers (Iglesias & Rogers 1993). This does cause some difficulty, however, since these tables do not extend to sufficiently high densities and temperatures for TNRs on massive WDs. When a mass zone is off the OPAL tables, we then switch back to the Iben analytic fits (see Iben & Renzini 1983 and references therein; we are grateful to I. Iben for providing us with these opacity fits) to the Cox opacities (Cox & Stewart 1971; Cox & Tabor 1976). While we do not smooth the transition between the OPAL opacities and the Iben fit opacities, the discontinuity does not seem to have caused any problems in the evolution. In fact, during most of the evolution, the transition from OPAL to Iben fit opacities occurs sufficiently deep into the envelope that the total opacity comes from electron degenerate conduction.

In addition to the above changes, we now use a value of α (the ratio of the mixing-length to pressure scale height: l/H_p) greater than one whenever a convective region exists. We do this because convection in WDs is known to be efficient and values larger than one have been found necessary for other studies of WDs such as the location of the ZZ-Ceti instability strip (Cox et al. 1987). In addition, a recent helioseismological analysis of the solar convective zone implies that α is close to 2.0 (Elliot 1996).

Our calculations were performed with 95 zone, $1.25\,M_\odot$, complete WDs since, as already mentioned, it appears that this value of the mass is a good choice for the mass of the WD in V1974 Cyg (Krautter et al. 1996). We chose only one WD mass for this study in order to concentrate on the effects of changing the opacities, nuclear reaction rates, and α on the evolution without adding the complications of also changing the WD mass. We varied the mass accretion rate and WD core temperature, when necessary, in order to produce evolutionary sequences that resembled the outburst of V1974 Cyg. As we will discuss in the next section, those sequences that were evolved with initial conditions identical to those used in Politano et al. (1995) resulted in TNRs but produced only slow nova-like behaviour.

We assume that the material being accreted from the donor star is of solar composition. We also assume, however, that mixing is taking place between the accreted material and the underlying WD

Table 2. Initial parameters and evolutionary results.

Sequence	1	2	3	4	4O	5	6	7	8
Mass	1.00M	1.25 $M_\odot$	1.25 $M_\odot$	1.25 $M_\odot$	1.25 $M_\odot$	1.25 $M_\odot$	1.25 $M_\odot$	1.25 $M_\odot$	1.35$M_\odot$
$\alpha(l/h_p)$	1.0	1.0	2.0	2.0	2.0	2.0	2.0	3.0	1.0
react. lib.	old	old	old	new	new	new	new	new	old
OPAL	no	no	no	no	yes	yes	yes	yes	no
$L/L_\odot(10^{-3})$	9.4	9.7	9.7	9.7	9.7	2.9	2.9	2.9	9.6
T_{eff} (10^4K)	2.0	2.6	2.6	2.6	2.6	1.9	1.9	1.9	3.0
Radius(km)	5379	3496	3496	3496	3509	3495	3495	3495	2488
M ($10^{-9}M_\odot yr^{-1}$)	1.6	1.6	1.6	1.6	1.6	1.6	.8	.8	1.6
τ_{TNR} (10^4 yr)	7.3	2.0	2.0	2.0	1.6	2.2	5.7	5.7	.9
$M_{acc}(10^{-5}M_\odot)$	10.5	3.2	3.2	3.2	2.5	3.4	4.5	4.5	1.5
$\epsilon_{nuc}(10^{17}$erg gm^{-1}s^{-1})	.2	1.0	1.1	1.1	0.8	1.3	1.4	1.2	1.9
T_{peak} (10^6K)	224	290	288	288	273	293	300	302	356
L_{peak} ($10^4L_\odot$)	2.2	4.3	7.6	6.1	4.4	10.5	11.7	15.0	16.3
$T_{eff-peak}$ (10^5K)	3.4	6.4	7.2	7.2	7.4	7.1	6.9	7.5	9.0
M_{ej} ($10^{-6}M_\odot$)	0	1	9.4	5.6	.3	2.0	4.6	6.6	5.2
V_{max}(km s^{-1})	45	560	1680	1450	430	1774	2080	2307	2320

by some, as yet, unknown mechanism. Guided by observations, therefore, we chose a composition for the accreting material that was enriched in oxygen, neon, and magnesium nuclei to 50 per cent (by mass). The remaining 50 per cent consisted of a solar mixture of the elements. The isotopic composition is given in Politano et al. (1995) and is derived from the carbon-burning nucleosynthesis calculations of Arnett & Truran (1969; see also Weiss & Truran 1990). We used the same initial composition for all our evolutionary sequences.

4 THEORETICAL STUDIES OF OXYGEN–NEON–MAGNESIUM NOVAE

Weiss & Truran (1990) and Nofar, Shaviv & Starrfield (1990), in separate and independent studies with different nuclear reaction networks but similar nuclear reaction rates, reported the results of their calculations which simulated the synthesis of ^{22}Na and ^{26}Al in ONeMg novae. Their calculations were performed with temperature, density and time profiles obtained from earlier hydrodynamic simulations of the outburst.

The general inferences drawn from the one zone nucleosynthesis studies must, however, be verified by hydrodynamic evolutionary studies. This provided the motivation for both Politano et al. (1995) and our present work. In an actual event, convective mixing carries material from the nuclear burning region to the surface on timescales of minutes, which is comparable to the positron decay timescales of the proton rich isotopes of carbon, nitrogen and oxygen. This increases the abundances of nuclei that would otherwise have been destroyed if they had not been transported to higher, cooler layers. In addition, convection continuously brings fresh nuclear fuel (e.g. in the form of ^{12}C and ^{16}O) from cooler regions close to the surface down into the nuclear burning layers, and keeps the nuclear reaction sequences operating far from equilibrium.

Our specific aim in this paper has been to explore the nuclear and hydrodynamic evolution, in response to a TNR, on a 1.25-$M_\odot$ white dwarf. We have used the best available nuclear reaction rates and opacities in order to determine if the outburst characteristics of Nova V1974 Cyg can be simulated by such a TNR. The results of our hydrodynamic calculations can be found in Tables 2 and 3. Table 2 gives the important parameters for both the initial models and the evolution, while Table 3 gives the predicted abundances for the most abundant elements in the ejecta. We record the abundances for all nuclei included in our network, and abundance information for the less abundant species is available from the authors. Sequences 1, 2 and 8 are identical to those given in Politano et al. (1995) and are provided here for ease of comparison. The values given in the rows of Table 2 are, respectively, the WD mass, the value of the convection parameter $\alpha(l/H_p)$ used for that sequence, the reaction rate library (old or new), the opacities used in the sequence (Iben fit or OPAL tables), the initial luminosity, the initial T_{eff}, the initial radius, the mass accretion rate, the runaway timescale, and the total amount of mass accreted. The next six rows give the values of the important parameters characterizing the evolution: the peak rate of energy generation and temperature, the peak luminosity and peak T_{eff}, the amount of mass ejected, and the maximum ejection velocity. Note that for sequences 1 through 5 we assumed that the rate of accretion on to the WD was 10^{17} g s^{-1} (1.6×10^{-9} $M_\odot$ yr^{-1}) and for sequences 6 and 7 we used 5×10^{16} g s^{-1} (8×10^{-10} $M_\odot$ yr^{-1}). The ejected mass reported is that amount which achieves escape velocity during the initial explosion. More material will be ejected later in the outburst by common envelope evolution and radiation pressure acting in combination, but a full study of that phase is beyond the scope of this paper.

4.1 Effects of increasing the convective efficiency

A significant problem with the 1.25-$M_\odot$ sequence, as reported in Politano et al., was that it ejected insufficient material moving at too low velocities to agree with the observations of V1974 Cyg. Since our choices of WD mass and envelope composition were guided by observations of this nova, these discrepancies were of particular interest. One way to increase both the mass ejected and the ejecta velocities is to increase the value of α used in the calculations. This increases the convective efficiency in the mixing-length algorithm that we use (Starrfield et al. 1978) which, in turn, increases the convective velocities and mixes more of the positron-unstable nuclei (and more of the nuclear energy associated with their decays) to the surface. It also mixes increased amounts of the stable, and still unburned, isotopes of the CNONeMg nuclei down

Table 3. Ejected abundances (by mass fraction).

Sequence	1	2	3	4	4O	5	6	7	8
Mass	1.00$M_\odot$	1.25 $M_\odot$	1.25 $M_\odot$	1.25 $M_\odot$	1.25 $M_\odot$	1.25 $M_\odot$	1.25 $M_\odot$	1.25 $M_\odot$	1.35$M_\odot$
X	0.33	0.30	0.30	0.31	0.32	0.31	0.31	0.26	0.27
Y	0.17	0.20	0.19	0.17	0.16	0.17	0.17	0.22	0.20
^{7}Be (10^{-8})	0.02	1.3	2.3	2.4	4.9	6.5	6.4	12.3	5.2
^{12}C	0.006	0.029	0.014	0.009	0.003	0.005	0.006	0.007	0.023
^{13}C	0.003	0.014	0.010	0.012	0.003	0.006	0.007	0.011	0.012
^{14}N	0.02	0.012	0.008	0.011	0.007	0.009	0.009	0.010	0.010
^{15}N	0.0001	0.012	0.037	0.054	0.052	0.064	0.065	0.064	0.076
^{16}O	0.095	0.025	0.023	0.016	0.027	0.017	0.015	0.014	0.005
^{17}O	0.023	0.045	0.050	0.038	0.056	0.045	0.040	0.036	0.006
^{18}O (10^{-4})	5.8	14.3	9.9	2.0	0.27	0.34	0.43	0.32	5.9
^{19}F (10^{-5})	2.5	2.4	1.9	1.4	1.9	2.8	2.9	1.7	4.5
^{20}Ne	0.25	0.23	0.23	0.23	0.23	0.22	0.22	0.22	0.17
^{21}Ne (10^{-5})	0.6	4.2	6.6	8.3	10.0	9.4	9.0	8.6	5.6
^{22}Ne (10^{-6})	22.9	2.4	1.2	0.7	2.3	0.54	0.42	0.39	0.8
^{22}Na (10^{-4})	0.5	7.6	6.1	17.2	22.9	30.2	32.7	20.3	55.4
^{24}Mg (10^{-4})	8.9	8.4	7.6	0.6	.59	1.1	1.3	0.92	13.9
^{25}Mg	0.058	0.037	0.036	0.003	0.003	0.005	0.006	0.005	0.039
^{26}Mg (10^{-3})	.08	1.2	1.2	0.2	0.3	0.59	0.66	0.43	3.7
^{26}Al (10^{-3})	19.6	9.5	10.1	1.2	0.5	1.0	1.3	1.7	7.5
^{27}Al	0.014	0.016	0.016	0.010	0.008	0.012	0.013	0.013	0.019
^{28}Si	0.016	0.046	0.047	0.084	0.089	0.077	0.073	0.078	0.032
^{29}Si (10^{-3})	0.1	2.5	2.2	2.8	3.5	4.0	4.0	3.1	4.1
^{30}Si (10^{-3})	0.04	10.0	9.5	21.0	14.4	18.0	19.2	20.0	17.4
^{31}P (10^{-4})	0.02	40.0	35.0	95.0	57.2	101.	112.	108.	202.
^{32}S (10^{-4})	1.1	30.0	21.0	76.0	31.3	75.4	88.0	81.2	290.
^{36}Ar (10^{-5})	1.9	2.1	2.1	0.54	0.79	0.51	0.45	0.43	41.0

into the region of peak nuclear burning which, for these models, is located at (or near) the core–envelope interface (hereafter, CEI). Increasing the numbers of radioactive nuclei at the surface and the heat transport to the surface, therefore, raises the surface temperatures and luminosities to higher values than found in simulations using a smaller value of α.

That this is exactly what happened can be seen by comparing the results for sequences 2 and 3 in Table 2. Sequence 3 was identical to sequence 2, except that α was chosen to be 2.0 instead of 1.0. Sequence 3 ejected $\sim 10^{-5}\,M_\odot$ at velocities up to 1700 km s^{-1} while sequence 2 ejected $\leq 10^{-6}\,M_\odot$ at velocities of only $\sim$550 km s^{-1}. In addition to the increases in the mass and velocity of the ejecta, the composition of the ejected matter also changed. The amount of ^{7}Be almost doubled, and the neutron-rich CNO isotopes increased in abundance (except for ^{13}C). These changes in abundance are due, in part, to the increased heating of the outer layers, which triggered a faster expansion and caused convection to retreat more rapidly from the surface regions. Since we have now established that a significantly better fit to the observations of V1974 Cyg can be obtained with the choice of a higher, but equally acceptable choice of α, we adopt this choice, α=2, as we explore the effects of the new reaction rates and opacities.

4.2 Effects of the new nuclear reaction rates

Sequence 4 was evolved with initial conditions identical to those used in sequence 3. The only change between these two simulations was the use of the updated nuclear reaction rates described in Section 3. As can be seen by examining the material in Van Wormer et al. (1994) and Herndl et al. (1995), there have been significant changes in many of the rates in the Ne–Mg–Al mass range (and above) from those published by Fowler and his collaborators (see, for example, Fowler, Caughlan and Zimmermann 1967, 1975; Wallace & Woosley 1981; Harris et al. 1983; Caughlan & Fowler 1988).

The early stages of the evolution of sequence 4 are virtually identical to sequence 3, as should be the case, since the important changes in the nuclear reaction rates occurred mainly for the intermediate-mass nuclei, and not for the nuclei that participate either in the proton–proton chain or the CNO cycle reaction sequences that determine the rate of energy generation and power the TNR. Differences do not show up until after peak temperature is reached. Fig. 1 shows the variation in the temperature of the deepest hydrogen-rich zone (in this simulation it is at the CEI, but this is not always the case) as a function of time near the time of peak temperature. The dashed line shows the temperature from sequence 3 and the solid line shows the temperature from sequence 4. We do not display the variation in energy generation rates for these models (the peak value for each model is given in Table 2) but the peak rate of energy generation occurs about 100 s before peak temperature and the rate of energy generation is already declining by the time that peak temperature occurs in the evolution. The changes in the nuclear reaction rates have caused less energy to be produced at the time of peak temperature in sequence 4 (as compared to sequence 3) and the temperature falls more slowly in this sequence. This is because less energy is being produced at the time of maximum temperature and there is less energy being convected to the surface. The reduced heating slows the expansion of the outer layers and the pressures and densities remain higher throughout the envelope as compared to sequence 3.

Fig. 2 shows the variation of $T_{\rm eff}$ on the same time-scale as used in Fig. 1. The solid line is the variation of $T_{\rm eff}$ from sequence 4 and the dashed line is from sequence 3. Fig. 2 shows that $T_{\rm eff}$ begins its rise almost simultaneously with the rise in temperature at the CEI and

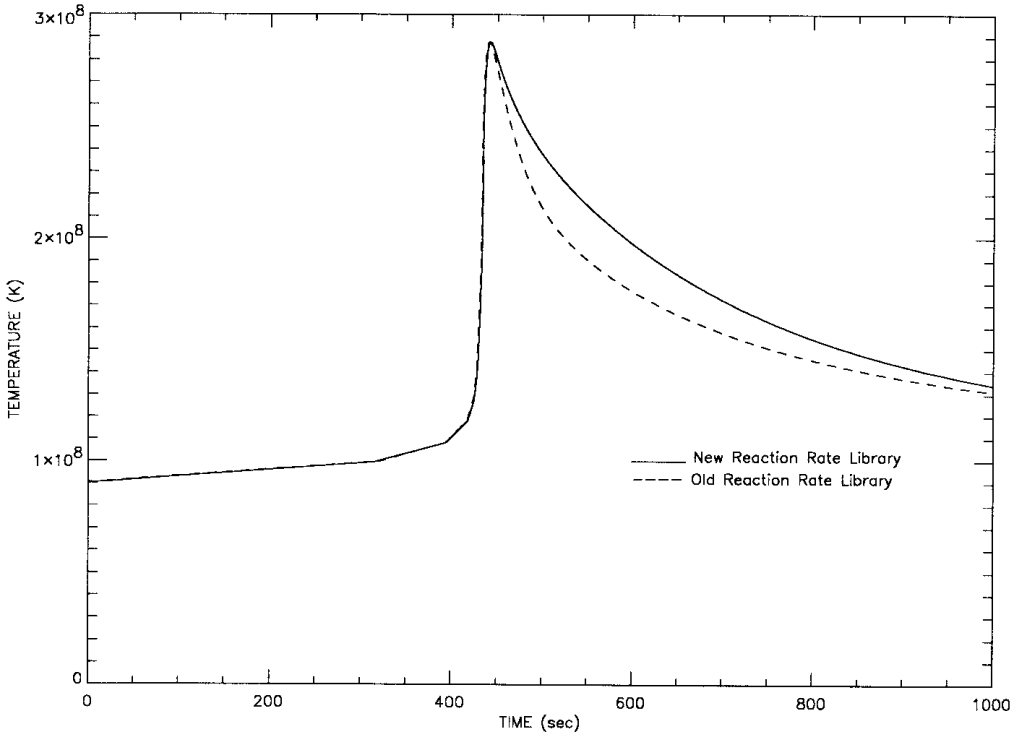

Figure 1. The variation with time of the temperature in the deepest hydrogen-rich zone near the peak of the outburst for two different sequences. The dashed line is the temperature from sequence 3 and the solid line is the temperature from sequence 4.

demonstrates how rapidly both the thermal energy and the positron-unstable nuclei are transported to the surface from regions near the CEI. Because less heat is produced in this sequence, however, the layers expand more slowly and $T_{\rm eff}$ drops more slowly. Within a few seconds after maximum $T_{\rm eff}$ has occurred, the top of the convective region has withdrawn from the surface layers to a few mass zones below these layers and the nuclear burning products from the deep interior no longer reach the surface (this also occurred in sequence

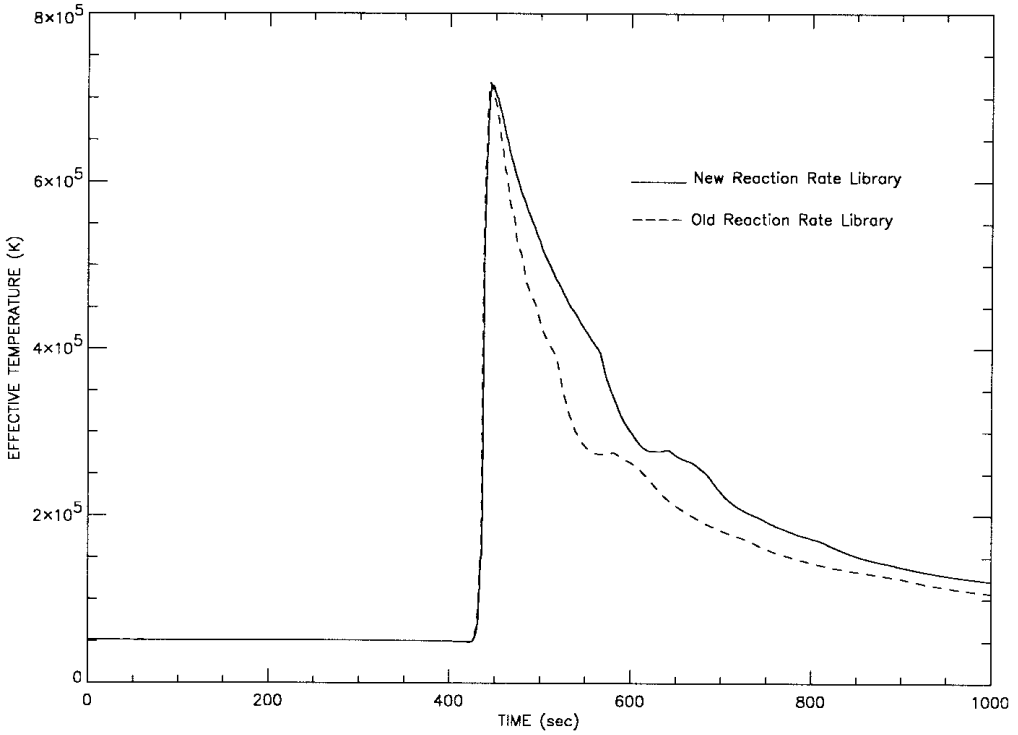

Figure 2. The variation with time of the effective temperature around the time when peak temperature is achieved in the TNR. The time-scale is identical to that shown in Fig. 1 and shows how rapidly the nuclear burning products from the depths of the hydrogen burning shell source reach the surface. The dashed line is the effective temperature from sequence 3 and the solid line is the effective temperature from sequence 4.

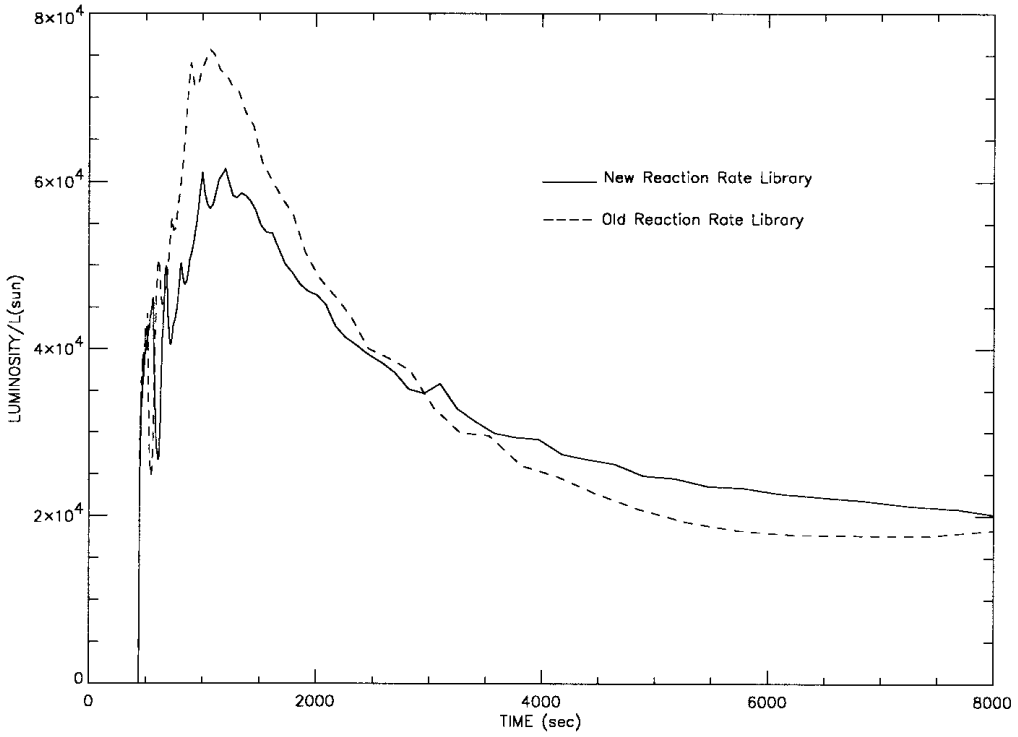

Figure 3. The variation with time of the surface luminosity for sequence 3 (dashed line) and sequence 4 (solid line). The beginning of the steep rise occurs at the same time that the effective temperature is rising to maximum. The oscillations are discussed in the text. The result of changing to the new reaction rates is to produce less energy at maximum temperature, which strongly effects the maximum luminosity.

3). This can also be seen in Fig. 3, which shows the surface luminosity variations over a two-hour period (beginning at the time of peak temperature) for both sequences 3 (dashed line) and 4 (solid line). Clearly, sequence 3 reaches a higher luminosity than sequence 4. Again, the cause is that less energy is produced during the epoch of peak burning.

The initial explosion drives the material to velocities of a few hundred km s^{-1} and the expanding gases then coast outward with slowly decreasing velocity. The surface layers are radiative, and the decreasing temperature and density in each mass zone causes an increase in the opacity by a factor of about two when the radius of each zone exceeds a few times 10^{10} cm. This increase in opacity reduces the Eddington luminosity in the zone to below the local luminosity and the zone velocity increases. Therefore, it is radiation pressure that accelerates the zones to velocities $\sim$1500 km s^{-1} in sequence 4 and $\sim$1700 km s^{-1} in sequence 3. The oscillations in the rising part of the light curve are caused by opacity effects. They occur at about the same time in each sequence and each of the oscillations is covered by many time steps so they are not caused by numerical instabilities but by point-to-point variations in the tabulated and coarsely zoned opacities.

Peak bolometric luminosity in sequence 4 occurs when the expanding material has reached $\sim 8 \times 10^{10}$cm. At this time, the energy generation in the surface layers has decreased to $\sim 10^{11}$ erg g^{-1} s^{-1}, and the heating produced by the positron decays is no longer sufficient to overcome the adiabatic cooling as these layers expand. By 8000 s after peak temperature, the luminosity has fallen to $\sim 2 \times 10^4\,L_\odot$, the outer radius has reached $\sim 10^{12}$ cm, and the surface zones are becoming optically thin. Fig. 4 shows the evolution of the two sequences in the theoretical Hertzsprung–Russell (HR) diagram. The entire evolution, from the time of peak temperature at the CEI to the time at which the surface has cooled to a $T_{\rm eff}$ of 10 000 K, takes less than 3 h. The surface zones are now expanding ballistically and the outermost $\sim 5 \times 10^{-7}\,M_\odot$ have reached escape velocity.

The abundances of various isotopes in the ejected material can be found in Table 3. The most interesting changes with respect to the abundances published in Politano et al. (1995), are that the abundance of ^{22}Na has increased from 6.1×10^{-4} (by mass: all abundances in this paper are given in mass fraction) to 1.7×10^{-3} and the abundance of ^{26}Al has *decreased* from 1.0×10^{-2} to 2.0×10^{-3}. The magnitude of these changes makes it clear that new calculations of nucleosynthesis associated with ONeMg novae, for plausible values of the WD mass $\sim$ 1.1–1.4 $M_\odot$, are warranted. An exploratory survey of such nucleosynthesis has recently been performed (Wanajoh, in preparation; see also Wanajoh, Nomoto & Truran, in preparation).

4.3 The effects of changing the opacities

Sequence 4 now represents the standard case with respect to which our further model sequences are to be compared since we have seen that the main effect of the inclusion of the updated nuclear reaction library has been only to modify the abundances in the material ejected in the early phases of a nova outburst. We wish now to explore the effects of the inclusion of the new OPAL opacities. To this end, we first calculated an evolutionary sequence with the same initial conditions used in our standard sequence (sequence 4), the only change being that we used the OPAL carbon-rich opacities (Iglesias & Rogers 1993). Sequence 4O(pal) accreted only about 80 per cent of the amount of material accreted by sequence 4. This is because the OPAL opacities, for the same density and temperature, are higher than the opacities provided by the Iben fit. The runaway time-scale for the TNR depends on the rate of energy transport out of the nuclear burning region, the peak of which is at the CEI. Since a larger opacity 'traps' more heat in the deeper layers, the temperatures

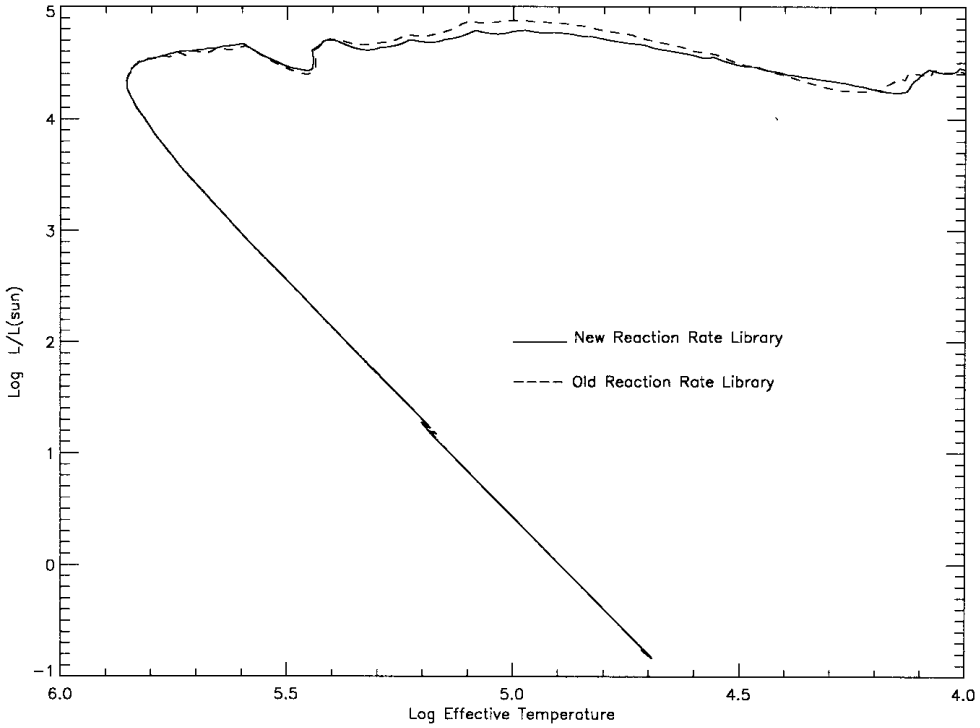

Figure 4. The evolution of sequence 3 (dashed line) and sequence 4 (solid line) in the theoretical HR diagram. It takes these two sequences less than 3 hours to evolve from minimum to an effective temperature of 10 000 K. By this time the radiative acceleration has ended and the escaping zones are expanding ballistically.

increase more rapidly in the deeper layers than found in our previous studies with the Iben opacity fits to the Cox opacities (Starrfield et al. 1992a; Politano et al. 1995). As discussed below, an important implication of this result is that metallicity plays a role in the outburst.

The results for sequence 4O are also given in Table 2. It reached a peak temperature in the envelope of $\sim 2.70 \times 10^8$ K and peak nuclear energy generation of $\sim 8 \times 10^{16}$ erg g^{-1} s^{-1}. These values are somewhat smaller than those achieved in sequence 4. Fig. 5

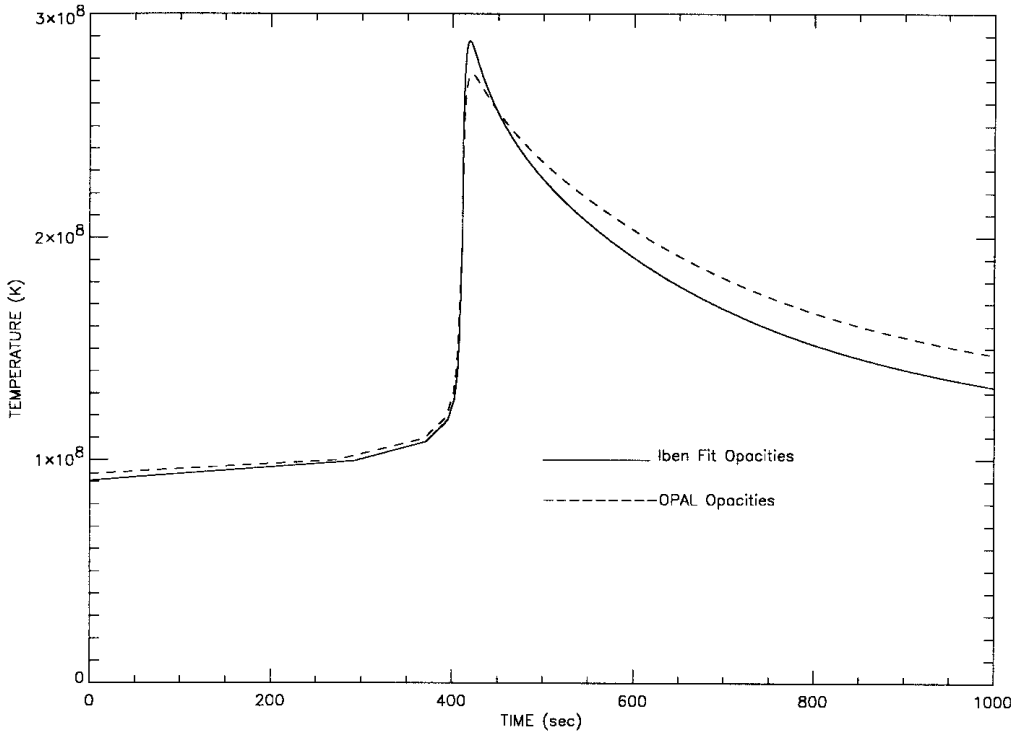

Figure 5. The variation with time of the temperature in the deepest hydrogen rich zone as a function of time for sequence 4 (solid line) and sequence 4O (dashed line). The horizontal scale was chosen to highlight the time when peak temperature is reached in the TNR.

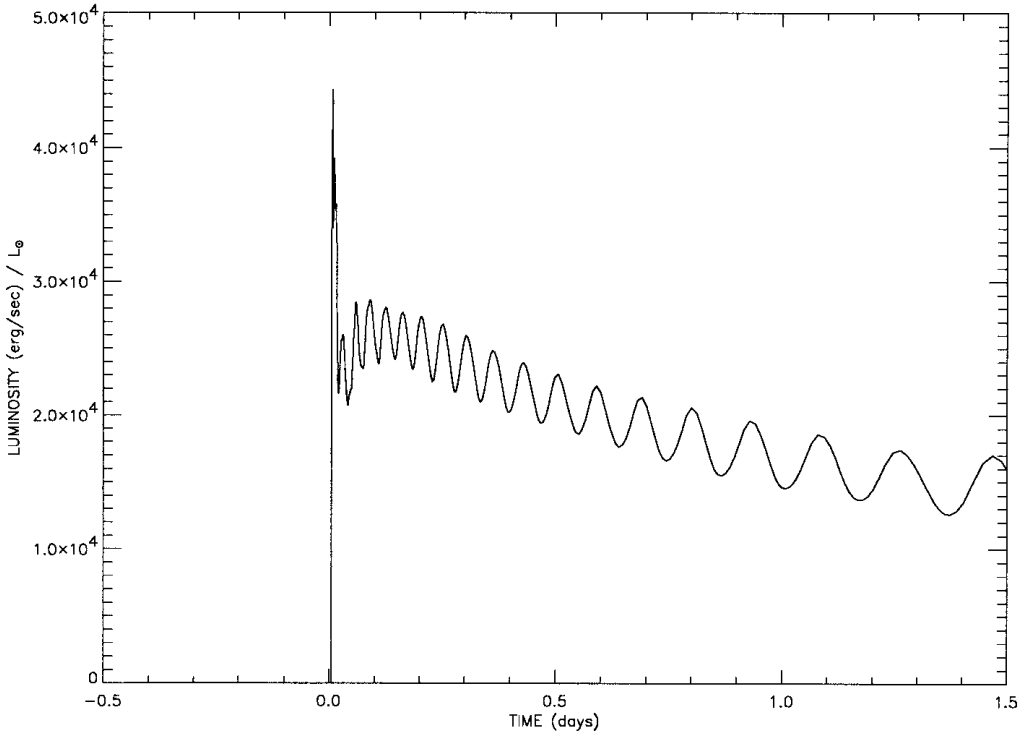

Figure 6. The surface luminosity as a function of time for sequence 4O. The beginning of the steep rise occurs simultaneously with the arrival of the convective region at the surface. The oscillations are real and are discussed in the text. Note how the period increases as the envelope expands.

shows the variation of the temperature with time at the CEI for both sequence 4 (the solid line) and 4O (the dashed line). The temperature falls more slowly in sequence 4O because less energy was being produced at the time of peak temperature, and the zones are expanding and cooling more slowly than in sequence 4.

The velocities, early in the evolution, were only $\sim$430 km s^{-1} and only $\sim 3\times10^{-7}$ M$_\odot$ were ejected in the early phases of the outburst. The peak luminosity for this sequence was $\sim 4.4\times10^4$ L$_\odot$. The material began expanding and about five hours after peak temperature in the TNR the outer layers had reached a radius of $\sim10^{12}$ cm and were moving with velocities of $\sim$450 km s^{-1}. At this time the luminosity had fallen to $\sim 2.2\times10^4$ L$_\odot$. An interesting result was that the region where nuclear burning was still proceeding extended from the radius of the CEI (3.5×10^8 cm) to a radius of $\sim 1.3\times10^{10}$ cm. This implies that the secondary will orbit within the rekindled nuclear burning region of the WD in short period nova binaries.

Fig. 6 shows the luminosity as a function of time for the first 1.5 d after the TNR. The sharp rise in luminosity occurred at the time that peak temperature was achieved at the CEI. The outer layers began pulsating in luminosity shortly after they reached a radius of a few times 10^{12}cm. The oscillations occurred only in the luminosity; the outer radii continued to expand and $T_{\rm eff}$ continued to drop during the entire 1.5 d shown in this plot. We note, however, that the point in the expanding flow where $T_{\rm eff}$ is determined is not fixed in mass but moves inward as the zones become optically thin.

We stopped the evolution about 1.5 d after peak temperature when the outer layers had reached a radius of $\sim 2\times10^{13}$ cm and were expanding ballistically. In addition to the material that was ejected during the explosive phase of the outburst, $\sim 6\times10^{-6}$ M$_\odot$ had radii greater than 10^{11} cm and would have been ejected by common envelope evolution. We note that the luminosity reached only $\sim 0.9L_{\rm Edd}$ (solar mixture, electron scattering opacity) so that it would appear that radiation pressure was unimportant in driving mass loss.

That this is not the case, however, has been shown in an important series of papers by Hauschildt et al. (1992, 1994a,b, 1996) who found that the very large opacity from the iron group elements ('iron' curtain), in a spherical, expanding, medium reduces the 'effective' Eddington luminosity by factors of as much as 100. This implies that radiation pressure is sufficient to drive off a significant fraction of the envelope when the iron group opacity is largest which occurs around the time of maximum light in the optical (Shore et al. 1994). The *expanding*, iron group, opacity is not in the OPAL tables and was not included in our calculations. We expect, however, that if it were included, then a larger fraction of the accreted envelope would have been ejected during the outburst.

Clearly, even though this sequence demonstrated a rise in brightness and ejected a small amount of material, its evolutionary characteristics did not resemble the observed behaviour of either V1974 Cyg or any of the other ONeMg novae observed up to now. Such novae are observed to become brighter at maximum, to eject more material (by factors of 100 or more), and to decline more rapidly. The observational consequences of the inclusion of the OPAL opacities are substantial. They suggest that we must find an alternative means of insuring that a larger amount of matter is accreted and ejected. There are two ways to accrete larger envelope masses prior to runaway: (1) lower the intrinsic white dwarf luminosity; and (2) lower the mass accretion rate.

4.4 Effects of lowering the white dwarf luminosity and the mass accretion rate

In order to increase the amount of accreted material, we lowered the surface luminosity of the initial model by a factor of 3 (to $L = 2.9\times10^{-3}$ L$_\odot$). This, in turn, lowered the core temperature

to $\sim 10^7$ K and reduced the temperatures near the outer edge of the WD so that $T_{\rm eff}$ decreased from $\sim$26 000 K to $\sim$19 000 K. This value is in better agreement with observations of WDs in nova systems (Sion, private communication; Shore et al. 1997). We accreted at the same rate as in sequences 4 and 4O but, because of the smaller interior temperatures, it took this sequence (sequence 5) about 50 per cent longer than sequence 4O to reach TNR conditions. The results of the evolution for sequence 5 are given in Tables 2 and 3. It reached a peak temperature of 2.93×10^8 K. This value was significantly larger than we found for sequence 4O and 5×10^6 K larger than sequence 4. Similarly, both peak nuclear energy generation and peak luminosity were larger than in sequence 4 and significantly higher than 4O.

We also found that sufficient numbers of positron decay nuclei reached the outermost zones to drive the peak rate of energy generation in the surface layers to more than 10^{15} erg g^{-1} s^{-1} for a few seconds after peak temperature was reached in the TNR. Therefore, there is a brief episode of γ-ray emission from electron–positron annihilation (Starrfield et al. 1992b). The intense heat from the positron decays, which occurred throughout the envelope, caused it to begin expanding. In addition, the luminosity in the outermost layers exceeded $L_{\rm Edd}$ by factors of two to three for more than 1000 s after the peak of the TNR. This rapidly accelerated these layers to velocities of 1600 km s^{-1}. The outermost layers reached a radius of 10^{11} cm about 930 s after peak temperature and by this time more than 4×10^{-7} M$_\odot$ had reached escape velocity. It took nearly two hours for the expanding gas to reach 10^{12} cm, at which time more than 1.4×10^{-6} M$_\odot$ were escaping (their velocities exceeded the escape velocity at that radius).

Shortly after the expanding layers reached a radius of 2×10^{12} cm, the outermost regions became optically thin and the photosphere began to move inward in mass. The temperature of this material had dropped to 12 000 K and the velocities had increased to more than 1750 km s^{-1}. We ended this evolution when the outermost zones had expanded past a radius of 6×10^{13} cm, which occurred about four days past peak temperature. At this time more than 2×10^{-6} M$_\odot$ had reached escape velocity and about 7×10^{-6} M$_\odot$ extended past a radius of 10^{11} cm and would probably have been ejected by a combination of common envelope evolution and radiation pressure. We also found that the region where nuclear burning was still proceeding extended from the radius of the CEI to $\sim 7 \times 10^9$ cm.

We emphasize that if we compare the mass of the *accreted* material in this sequence to the determinations of the masses of the ejected matter associated with the outbursts of QU Vul or V1974 Cyg [$\sim 5 \times 10^{-4}$ M$_\odot$(Saizar & Ferland 1994) and 1 to 5×10^{-4} M$_\odot$ (Austin et al. 1996; Hayward et al. 1992; Woodward et al. 1997)], we fall short by factors of order two to 10. In order to increase the amount of accreted, and ejected, gas over that in sequence 5, we decreased the mass accretion rate and evolved a new sequence.

Sequence 6 had the same initial conditions as sequence 5 but the mass accretion rate was reduced to 8×10^{-10} M$_\odot$ yr^{-1} (half that of sequence 5). Sequence 6 took 57 500 yr to reach the peak of the TNR and accreted an envelope mass of 4.5×10^{-5} M$_\odot$. This value is close to the amount of *ejected* gas determined for V1974 Cyg (Austin et al. 1996; Shore et al. 1993). We ended the accretion phase when the temperature of the CEI had reached $\sim 3.5 \times 10^7$ K. At this time, the rate of energy generation had reached $\sim 1.1 \times 10^8$ erg g^{-1} s^{-1} and the zones were expanding at speeds of 0.02 cm s^{-1} .

It took about 142 d for the mass zone just above the CEI to evolve from a temperature of 3.5×10^7 K to 10^8 K, and for the nuclear energy generation to increase to 5.5×10^{13} erg g^{-1} s^{-1}. At this stage, the surface layers were expanding at a velocity of 0.2 km s^{-1}. Unlike the previous sequences that we have discussed in this paper, the actual mass zone in which the TNR occurred was one zone above the CEI. The low accretion rate on to the massive WD had increased the degeneracy at the CEI to a value where conduction into the interior was sufficient to keep the zone at the CEI too cool to experience a TNR.

The evolutionary results for sequence 6 can be found in Table 2. This sequence reached a peak temperature, one zone above the CEI, of 3.00×10^8 K and a peak rate of energy generation exceeding 1.4×10^{17} erg g^{-1} s^{-1}. Shortly after peak temperature was achieved, sufficient heat and positron decay nuclei had reached the surface to raise the nuclear energy generation in the outermost layers to $\sim 1.3 \times 10^{15}$erg g^{-1} s^{-1} and the $T_{\rm eff}$ to nearly 7×10^5 K. The intense heat released within the surface layers caused them to rapidly accelerate outward and, within a few minutes after peak $T_{\rm eff}$, these layers had reached velocities exceeding a few hundred km s^{-1}. This sequence ultimately ejected $\sim 5 \times 10^{-6}$ M$_\odot$ moving at velocities exceeding 2000 km s^{-1}. This is significantly less material than was ejected by sequence 3 but nearly equal to that ejected by sequence 4. We ended the evolution when the outermost zones had reached radii of $\sim 10^{15}$ cm. Clearly, the characteristics of this evolution are in better agreement with the observations of V1974 Cyg although differences remain.

4.5 Effects of increasing the convective efficiency revisited

In an attempt to produce an even stronger outburst, using both the new reaction rates and the OPAL opacities, we evolved another sequence with the same initial conditions as those of sequence 6 but with α = 3. The results are again given in Table 2 and the ejecta abundances can be found in Table 3. The initial evolution is very similar to that of sequence 6. Again, as in sequence 6, peak nuclear burning does not occur at the CEI but one zone closer to the surface. Since convective mixing is more efficient, however, larger numbers of 'unburned' ONeMg nuclei are brought down to the region of peak burning from the surface layers, and peak energy generation is higher in this sequence than in sequence 6. In contrast, peak temperature is lower. This is exactly the same situation that we found when we compared sequence 3 with sequence 2. The increased heating throughout the accreted envelope caused the surface layers to expand earlier, which reduced the pressure in the region of peak nuclear burning; and, in turn, decreased the temperature.

We end accretion in sequence 7 when the temperature, one zone above the CEI, has reached 5×10^7 K and the nuclear energy generation has reached $\sim 2 \times 10^{10}$ erg g^{-1} s^{-1}. At this time the surface zones are expanding at about 100 cm s^{-1}. These values are slightly different from those given for sequence 6 and mark the switch from evolution with our accretion algorithm to constant mass evolution. The change in α caused the two sequences to evolve differently once convection was initiated at a temperature of $\sim 3 \times 10^7$ K. We prefer not to rezone at a time when the temperature, mass accretion rate, and abundances are changing rapidly. At the time that we make the switch we are less than a week away (sometimes only a day) from peak temperature. The differences in the values at the time of switch-over are an insignificant fraction of the evolution time of 10^4 yr.

It takes this sequence another 0.5 d for the peak temperature in the nuclear burning zone to reach 10^8 K. The variation with time of the total nuclear luminosity (in solar luminosities and integrated

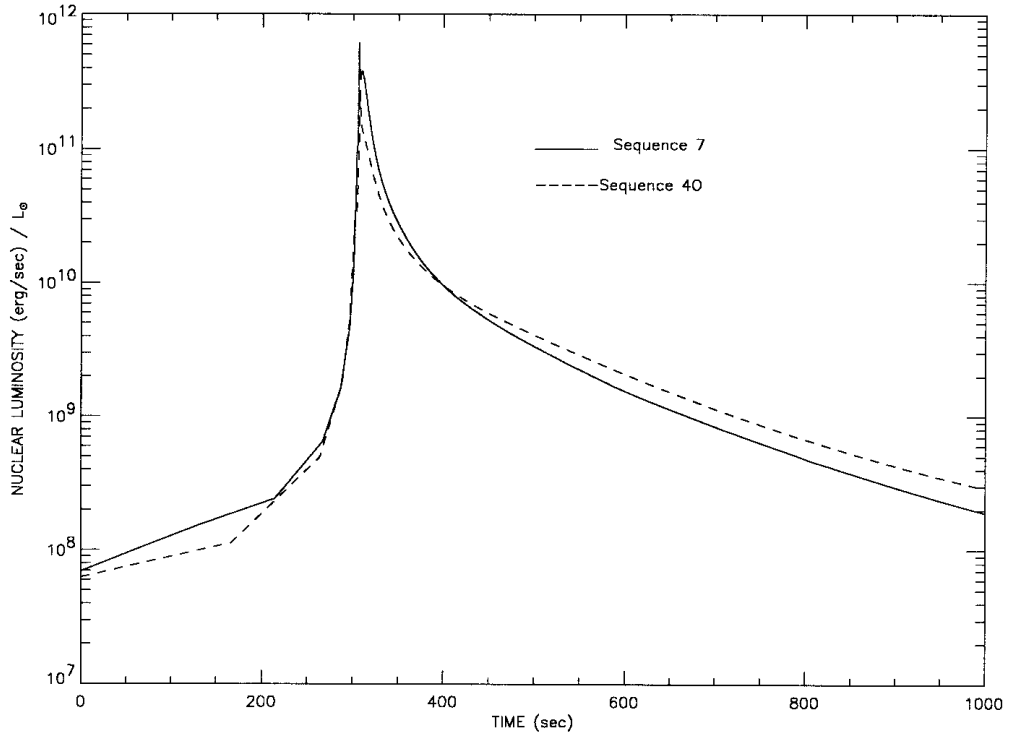

Figure 7. The variation with time of the nuclear luminosity (in solar luminosities) around the time of peak temperature in the TNR. We have integrated over all zones taking part in the TNR so that each point gives the total nuclear luminosity produced at a given time-step. The solid line is for sequence 7 and the dashed line is for sequence 4O. The horizontal scale is the same as in Fig. 5 and comparison of these two plots shows that peak nuclear energy generation occurs before peak temperature.

over the accreted envelope) is shown in Fig. 7 for both sequence 7 (the solid line) and 4O (the dashed line). Note that it grows by nearly 4 orders of magnitude in less than 100 s.

The luminosity falls more rapidly in sequence 7 than in sequence 4O because more energy is produced at peak energy generation in sequence 7, so that the zones expand and cool more rapidly. By the time that peak energy generation is reached in sequence 7, a very strong convective region has grown to the surface and is carrying both heat and positron unstable nuclei to the outermost layers. This causes $T_{\rm eff}$ to rise rapidly to $\sim$750 000 K. The variation of $T_{\rm eff}$ with time for both sequence 7 (solid curve) and sequence 6 (dashed curve) is shown in Fig. 8. It is plotted on the same time-scale as in Fig. 7. In Fig. 9 we show the luminosity as a function of time for both sequence 7 (solid curve) and 6 (dashed curve) over the first 4 h of the outburst. Note that in both sequences peak luminosity exceeds $L_{\rm Edd}$ by nearly an order of magnitude. Fig. 10 shows the evolution of both sequences in the theoretical HR diagram (the evolution of sequence 7 is given by the solid curve and 6 by the dashed curve). It takes about 10 s for these sequences to evolve from minimum temperature to peak temperature and then another 2 to 3 h to cool to a temperature of 10^4 K.

The results of these two sequences, one with $\alpha = 2$ and the other with $\alpha = 3$, show that increasing the convective efficiency strengthens the outburst. Sequence 7 ($\alpha = 3$) ejects more material at higher speeds than does sequence 6 ($\alpha = 2$). In addition, sequence 7 reaches a higher peak luminosity and, thereby, peak bolometric magnitude than does sequence 6. Nevertheless, the total ejected mass, $\sim 7 \times 10^{-6}\,{\rm M}_\odot$ and the peak luminosity are smaller than observed for the outburst of V1974 Cyg. Since it was our intent to model the outburst of V1974 Cyg, by concentrating on evolutionary sequences at $1.25\,{\rm M}_\odot$, we cannot claim total success. We also note that the amount of material ejected in sequence 7 is smaller than in sequence 3. Therefore, the major result of improving the physics included in our calculations has been to reduce the amount of ejected mass which, in turn, has driven our results farther from the observations.

5 NUCLEOSYNTHESIS CONSIDERATIONS

To the extent that sequence 7 provides the best fit to the observed behaviour of Nova V1974 Cyg in outburst, it is appropriate to examine some implications for nucleosynthesis. During the evolution to peak and beyond, the nuclear reactions in sequence 7 produce three important long-lived radioactive nuclei, in addition to the short-lived positron decay nuclei that are so important for the progress of the outburst. These nuclei are ^{7}Be and ^{22}Na, which may be detectable from nearby novae, and ^{26}Al which is important in studies of galactic nucleosynthesis (Nofar et al. 1991) and has been detected by the *Compton GRO* (Diehl et al. 1995). At the beginning of the sequence, these three nuclei have an abundance of zero. The initial abundance of ^{27}Al is set to 1.65×10^{-5} (mass fraction). We do not use the large network during the earliest stages of accretion and so the abundances of ^{26}Al and ^{22}Na are still zero at the beginning of the steep rise to peak temperature. The temperature, at this time, in the mass zone where the nuclear burning is largest (one zone above the CEI) is $\sim 5 \times 10^7$ K. The abundance of ^{7}Be, however, has grown to $\sim 2.6 \times 10^{-10}$ in the convective region but is still zero in the regions where convection has not yet reached. By the time that the temperature has climbed to $\sim 6.6 \times 10^7$ K (a little over three hours later), the abundance of ^{7}Be is 4.4×10^{-9}, that of ^{22}Na has reached $\sim 1.5 \times 10^{-4}$, ^{26}Al has reached $\sim 2.3 \times 10^{-6}$, ^{26m}Al (the isomeric state) has reached $\sim 5.2 \times 10^{-11}$, and that of ^{27}Al has reached $\sim 1.6 \times 10^{-5}$.

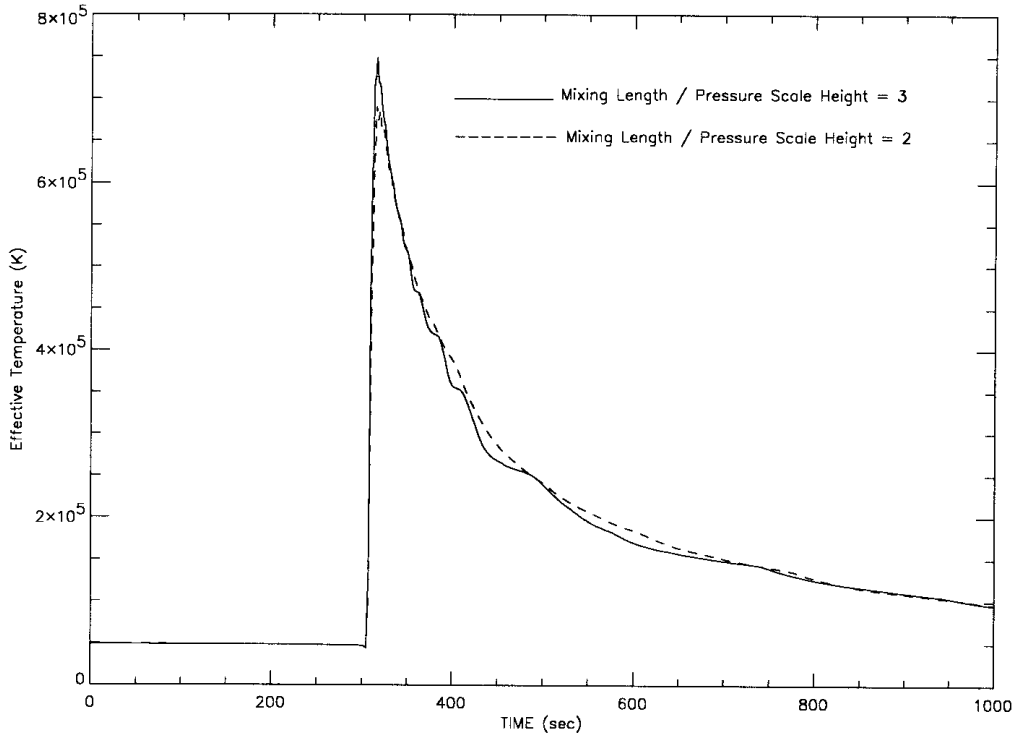

Figure 8. The variation with time of the effective temperature around the time when peak temperature is achieved in the TNR. The time-scale is identical to that shown in Fig. 5 and shows how rapidly the nuclear burning products from the depths of the hydrogen burning shell source reach the surface. The dashed line is the effective temperature from sequence 6 and the solid line is the effective temperature from sequence 7.

Over the next few seconds, the temperature climbs rapidly to a peak temperature exceeding 3.00×10^8 K (Table 2) and the abundances of ^{7}Be, ^{22}Na, ^{26}Al, ^{26m}Al, and ^{27}Al reach $\sim 2 \times 10^{-7}$, $\sim 2 \times 10^{-3}$, $\sim 1 \times 10^{-3}$, $\sim 5 \times 10^{-3}$, and $\sim 1 \times 10^{-2}$, respectively. In all cases, these abundances are averages over the convective region, which now extends almost to the surface. In the next few seconds, convection reaches the surface layers and the energy generation in the surface mass zone jumps to $\sim 1.5 \times 10^{15}$ erg g^{-1} sec^{-1}.

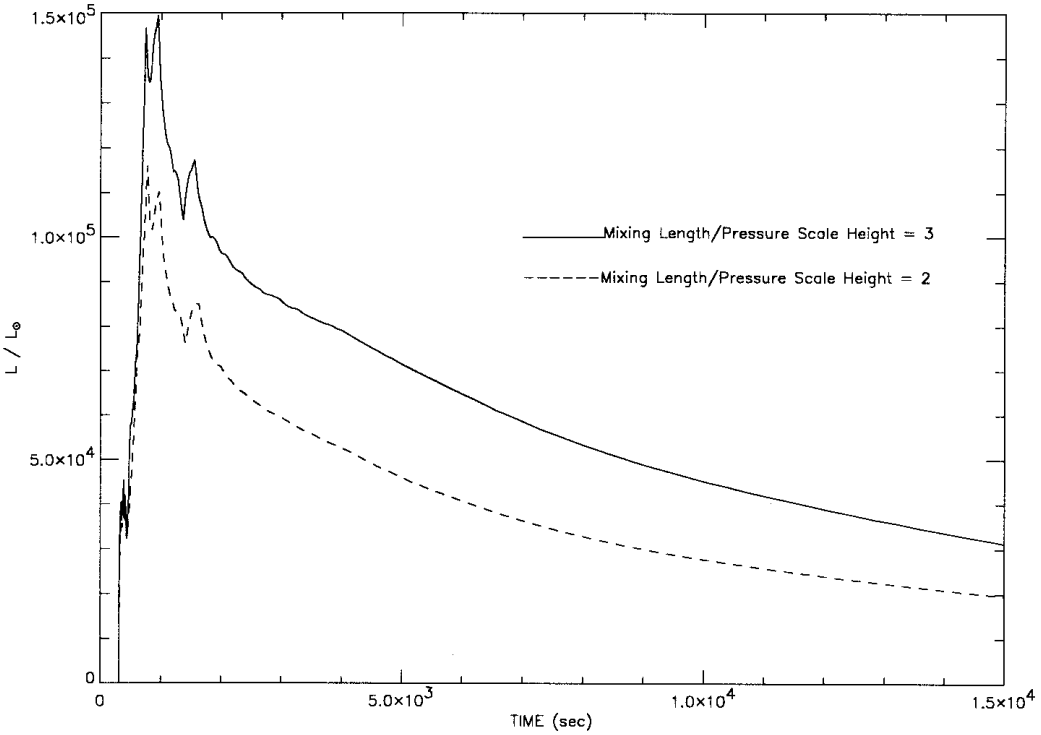

Figure 9. The variation in time of the surface luminosity for sequence 6 (dashed line) and sequence 7 (solid line) for the first few hours after peak temperature occurred in the TNR.

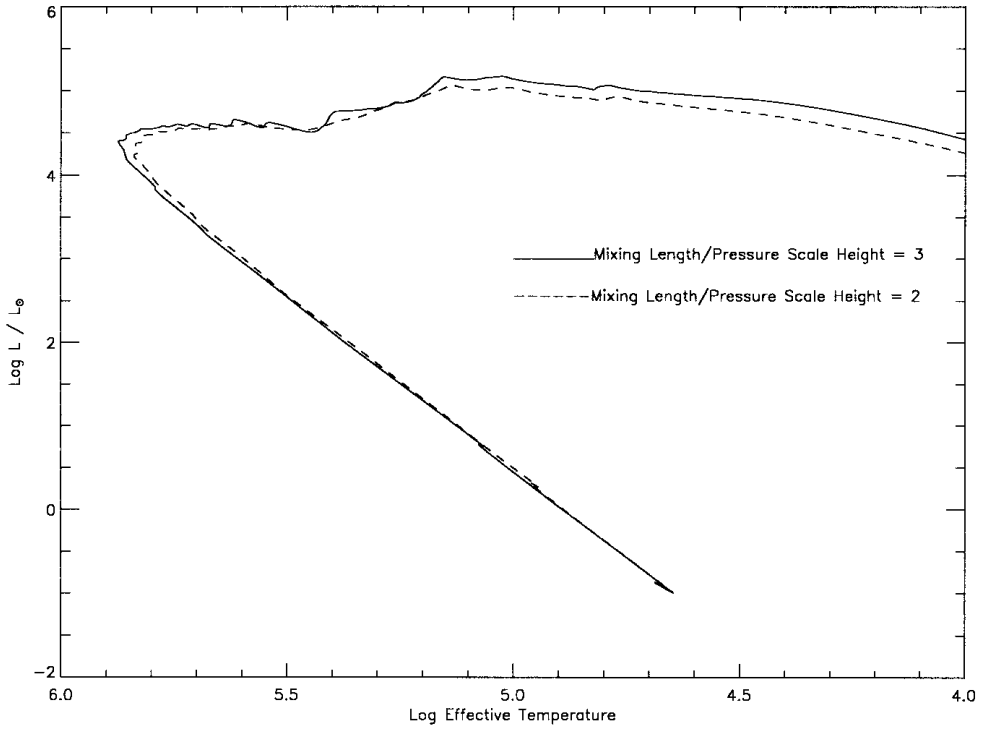

Figure 10. The evolution of sequence 6 (dashed line) and sequence 7 (solid line) in the theoretical HR diagram. It takes these two sequences about 10 s to evolve from minimum temperature to maximum temperature and then another 3 to 4 hours to an effective temperature of 12 000 K.

The temperature now declines very rapidly. It takes only 30 s for it to drop to 2.55×10^8 K while the expanding outer layers have reached $\sim 1.6 \times 10^9$ cm. The abundances of ^{7}Be, ^{22}Na, ^{26}Al, ^{26m}Al, and ^{27}Al are now: $\sim 1 \times 10^{-7}$, $\sim 5 \times 10^{-3}$, $\sim 4 \times 10^{-4}$, $\sim 3 \times 10^{-4}$, and $\sim 1.2 \times 10^{-2}$, respectively. The abundance of the isomeric state of aluminum has reached a maximum and it is now decaying to ^{26}Mg. It seems that at the high temperatures reached in our sequences, we make a large amount of ^{26}Mg via the decay of ^{26m}Al. At peak temperature, ^{25}Al(p,γ) ^{26}Si is faster than the ^{25}Al beta decay so that a large amount of ^{26}Si is formed. In addition, while ^{26}Si(p,γ) is about as fast as ^{25}Al(p,γ) ^{26}Si, the former reaction is suppressed by the inverse photo disintegration because of its low Q value. Therefore, it is ^{26}Si that is enriched. ^{26}Si then decays to ^{26m}Al, which in turn decays to ^{26}Mg, which proton-captures first to ^{27}Al and then to ^{28}Si. In contrast, ^{26}Al can only be made by ^{25}Mg(p,γ)^{26}Al and ^{25}Mg is only produced from the beta decay of ^{25}Al. Although ^{25}Al is directly produced by a proton capture on ^{24}Mg, ^{26}Al can only be produced when the temperatures are too low for proton captures on ^{25}Al.

Again, the abundance values that we quote are averages of the abundances in the convective region which still extends to the surface but, in the next few minutes, will begin to retreat inward in mass as the surface layers expand and cool. With our use of a time-dependant mixing algorithm, we do not completely homogenize the convective zone, and thus we find that the abundances of these nuclei vary throughout the accreted layers on the WD. The abundance of ^{7}Be is roughly constant, the abundance of ^{22}Na increases outward with mass (by a factor of 10), the abundance of ^{26}Al decreases outward, and the abundances of ^{26m}Al and ^{27}Al increase outward. By this time, the rate of energy generation at the surface has dropped to $\sim 10^{14}$ erg g^{-1} sec^{-1}.

660 s after peak temperature, the outermost zones ($\sim 10^{-6}$M$_\odot$) have reached a radius of nearly 9×10^{10} cm. The abundances of ^{7}Be, ^{22}Na, ^{26}Al, ^{26m}Al, and ^{27}Al in this region are now: $\sim 1 \times 10^{-7}$, $\sim 5 \times 10^{-3}$, $\sim 8 \times 10^{-4}$, $\sim 10^{-11}$, and $\sim 10^{-2}$, respectively. Because the abundances vary with depth in the region that was once part of the convective zone, the values given in Table 3 are different from these values. As more zones reach escape velocity, the abundances will change slightly to reach the values reported in Table 3.

6 COMPARISON WITH V1974 CYG 1992

As emphasized earlier, a primary purpose in performing this study was to compare the results of our simulations to the observations of the outburst of V1974 Cyg. Given that the mass of the WD is close to 1.25 M$_\odot$ (Krautter et al. 1996), the other parameters to compare are the amount of ejected mass, the abundances in the ejecta, the light curve and the kinetic energy of the ejecta. We give particular attention here to comparisons of abundances and the mass of the ejecta.

The observed abundances for V1974 Cyg are obtained from analyses of ultraviolet, optical, and infrared nebular emission line spectra (Austin et al. 1996; Hayward et al. 1996). Austin et al. used an optimization technique plus CLOUDY (Ferland 1996) to determine the abundances for H, He, N, O, Ne and Fe in the ejected material (see Table 4). Hayward et al. followed the mid-IR evolution of two emission lines and used CLOUDY plus the analysis of Austin et al. to determine the nebular abundances. We present in Table 4 the results of both studies plus the initial abundances and the resulting abundance patterns obtained in this study for sequences 6 and 7 (we have summed over the individual isotopic abundances to provide the total elemental abundances).

Comparison of the abundance patterns resulting from our simulations with those determined for the ejecta of V1974 Cyg reveals several interesting features. Note first that both observational studies (Austin et al. 1996; Hayward et al. 1996) find the helium

Table 4. Abundance comparison: two simulations with V1974 Cyg.

Element	Initial Abundance	sequence 6	sequence 7	V1974 Cyg[1] Austin	V1974 Cyg[2] Hayward
X	0.365	0.31	0.26	0.19	0.30
Y	0.133	0.17	0.22	0.32	0.52
C	9.5×10^{-4}	0.013	0.018		.016
N	3.2×10^{-6}	0.074	0.074	0.085	0.023
O	0.15	0.062	0.055	0.29	0.102
Ne	0.249	0.22	0.22	0.11	0.037
Na	9.2×10^{-6}	0.003	0.002		1.4×10^{-5}
Mg	0.10	0.007	0.005		0.0014
Al	1.6×10^{-5}	0.014	0.015		1.2×10^{-4}
Si	1.8×10^{-4}	0.10	0.10		0.0018
S	1.1×10^{-4}	0.009	0.008		7.8×10^{-4}
Ar	2.3×10^{-5}	4×10^{-6}	4×10^{-6}		2.6×10^{-4}

[1] Austin et al. (1996)
[2] Hayward et al. (1996)

mass fraction to be significantly greater than that of hydrogen. In contrast, our calculations for both sequences included in Table 4 yield $X > Y$, consistent with the burning of only 5 to 10 per cent of the hydrogen in the envelope to helium during the outburst (cf. Krautter et al. 1996). The observational findings, therefore, suggest the possibility of an initial helium (as well as heavy element) enrichment of the envelope. We shall return to this issue in the next section.

With regard to elements heavier than hydrogen or helium, the two studies yield different values of Z: 0.48 (Austin et al.) and 0.18 (Hayward et al.). This is perplexing since Hayward et al. based their analysis on only two IR lines and the results of Austin et al. Our initial abundance distribution [chosen for the study in Starrfield et al. (1992) which was carried out prior to the discovery of V1974 Cyg in outburst], a 50 per cent enrichment in matter from an underlying ONeMg WD, is clearly more consistent with the results of Austin et al. Note that both studies find significant levels of enrichment of Ne as well as O, a clear signature of an ONeMg WD. The fact that our simulations yield O/Ne < 1, whereas the observations indicate O/Ne > 1, may be related to our choice of the post-carbon-burning abundances of Arnett & Truran (1969). We hope to reduce this discrepancy by using oxygen–neon abundance distributions from either Nomoto & Hashimoto (1988) or Ritossa, Garcia-Berro & Iben (1996) who find that a larger amount of oxygen and smaller amount of magnesium are produced in $10\,M_\odot$ stars than reported in Arnett & Truran (1969). Table 4 also shows that while increasing the convective efficiency ejects more mass at higher velocities, it does not strongly affect the abundance results.

It is also appropriate to mention the considerable change in the argon abundance between the simulations with the old and new reaction rates. Part of the cause for this difference is that the new reaction rate of ^{36}Ar(p,γ) (Iliadis et al. 1992a,b) is several orders of magnitude larger than previously estimated (Wallace & Woosley 1981). This causes a rapid depletion of argon as compared to previous nova calculations (Starrfield et al. 1992a; Politano et al. 1995). However, there is still considerable uncertainty in the reaction rate of ^{35}Cl(p,α) for low temperatures (Iliadis et al. 1994; Ross et al. 1995). A recent study (Iliadis et al. 1997) indicates the possibility of an additional low-energy resonance in ^{35}Cl(p,α), which would trigger a SCl-cycle. Further experimental studies are necessary, however, to verify the contribution of this resonance level and it will be useful to obtain the abundances of more elements in this region of the periodic table.

Shore et al. (1993), Austin et al. (1996), and Hayward et al. (1996) obtained values for the ejected mass ranging from $\sim5\times10^{-5}\,M_\odot$ to nearly $\sim5\times10^{-4}\,M_\odot$. Our prediction for the amount of mass ejected during this early phase of the nova evolution (sequences 6 and 7) is more than a factor of 10 less than was observed. This alone is not too significant a problem, in that mass loss induced by common envelope interactions (MacDonald, Fujimoto & Truran 1983; Truran & Glasner 1995) and by radiation pressure driven winds, acting in combination, can increase the *total* mass ejected. It is of far greater concern that our simulations did not *accrete* as much mass (prior to runaway) as was observed to be ejected. It would again appear that improving the input physics in our simulations has worsened the conflict between our results and the observations, with respect to estimates of the total envelope mass (accreted and/or ejected) in representative nova explosions.

Finally, we emphasize that this is not a problem unique to V1974 Cyg. Observations of other ONeMg novae indicate that they are ejecting more material than theoretical considerations predict can normally be accreted. For example, the observations of V838 Her 1991 suggest that the outburst occurred on a WD with a mass $\sim1.35\,M_\odot$. Theoretical predictions imply that such a WD will accrete $\sim4\times10^{-6}\,M_\odot$ before the TNR occurs (Starrfield 1989; Gehrz et al. 1998). Observations of the outburst, however, indicate that somewhere between 10^{-4} and $6\times10^{-4}\,M_\odot$ were ejected during the outburst (Woodward et al. 1992; Vanlandingham et al. 1996). For another example, we refer to the outburst of QU Vul 1984 #2. Its outburst was very slow for an ONeMg outburst and we suggest that the explosion occurred on a 1.0-$M_\odot$ WD. Such a WD should be able to accrete about $1.3\times10^{-4}M_\odot$ before the bottom reaches a pressure of $\sim10^{20}$ dyn cm^{-2} (Starrfield 1989; Gehrz et al. 1998). The observations of QU Vul, however, imply that as much as $10^{-3}\,M_\odot$ could have been ejected if all the hot, diffuse gas had been included in the determinations (Saizar & Ferland 1994).

7 WHERE IS THE 'MISSING' MASS?

As discussed in the last section, our earlier evolutionary sequences did not eject sufficient material to agree with the observations. In this paper we have investigated the effects of improving both the nuclear reactions and the opacities used in our evolutionary calculations and find that the situation has worsened. While improvements in the nuclear reaction rates have made only slight changes to our earlier results (compare, for example, sequences 3 and 4), our use of the OPAL opacities has had substantial effects. In fact, we have been forced to lower both the initial WD luminosity and the rate of accretion, from our previous values, in order to approach the amount of mass ejected in Starrfield et al. (1992a) and Politano et al. (1995).

It is clear why this must be the case. 'Improving' the opacities implies that more levels and lines are included, more detailed broadening mechanisms are included, and the level populations are treated in a more realistic fashion (Rogers, Swenson & Iglesias 1996, and references therein). Virtually all of these changes act to increase the opacity at a given temperature and density when compared to older generations of opacity tables (cf. Cox & Stewart 1971; Cox & Tabor 1975). For our nova studies, increasing the opacity makes it easier to trap the heat produced by nuclear reactions at the CEI and so the temperatures rise more rapidly per unit accreted mass. This implies, in turn, that the accretion time is shorter and the amount of accreted mass lower than found in our

earlier studies. The results of these changes are only exacerbated when we realize that the admixture of core material into the envelope, which enriches the heavy-element mass fractions, also increases the opacity.

In this context, we see that the effect of an increased opacity is dependent upon precisely when and how the enriched material is inserted into the accreted material. Four mechanisms have been proposed and they are discussed in detail in Sparks et al. (1990) and Livio (1994). Two result in mixing during the entire accretion process: diffusion (Prialnik & Kovetz 1984; Kovetz & Prialnik 1985, 1994; Iben, Fujimoto & MacDonald 1991, 1992a, b; see also Iben 1992) and accretion-driven shear mixing (Kutter & Sparks 1987; Sparks & Kutter 1987). Diffusion can produce large enrichments if the accretion rate is low: $\sim 10^{-10}\,M_\odot\,yr^{-1}$ (or lower). The observed rates of mass accretion in classical novae, however, are about one to two orders of magnitude higher (Livio 1994, and references therein). The other two occur when convection is important. One is convective overshooting via flame propagation during the peak of the TNR (Woosley 1986) and the other is convection-driven shear mixing (Kutter & Sparks 1989). Although Woosley (1986) refers to the process as convective overshooting, in fact the physical process involves the penetration of convective elements below the lower boundary of the convective region. Therefore, we prefer to call this 'undershooting' in order to distinguish it from the motion of the elements above the convective region. The theoretical studies of convective undershooting are more developed than the theory of convection-driven shear mixing and recent two-dimensional studies imply that undershooting is an important physical process (Hurlburt et al. 1994) in the nova outburst (Glasner & Livne 1995; Glasner, Livne & Truran 1997; Kercek, Hillebrandt & Truran 1997).

We have assumed in our calculations that the accreting material was enriched to the desired level from the beginning of the accretion phase. This is what is expected from either shear mixing or diffusion. We did this because, previously, we did not have a preference for any of the proposed enrichment mechanisms and this method allowed us to calculate reproducible evolutionary sequences. It is this assumption, however, that is likely responsible for the small values of the accreted mass in both our simulations and those of Prialnik & Kovetz (1995) who assume that diffusion is occurring as the material is accreted.

Numerous studies of TNRs, which occur in the material accreted on to WDs, show that the phase which is important in determining the *total* amount of material that can be accreted prior to runaway is the proton–proton burning phase. It is this phase which occurs first because it proceeds at the lowest temperatures for any of the proton capture reactions. Because the temperature dependance of the proton–proton reaction sequence is low, $\epsilon_{\rm nuc} \sim T^{4-6}$, a major fraction of the nuclear energy produced by this sequence is radiated (along with the compressional energy produced by the accreting material). Therefore, the increase in temperature per unit accreted material is very small and the WD spends a major fraction of the accretion time in this phase. Once the temperatures have risen to about 10^7 K, the CNO cycle reactions, $\epsilon_{\rm nuc} \sim T^{16-18}$, begin to play an important role in the evolution and the TNR quickly (as compared to the time spent in the proton–proton phase) evolves to peak conditions.

As can be seen from our simulations, lowering the initial WD luminosity (and, thereby, the interior temperatures) decreases the initial rate of energy generation so that more time is spent in the proton–proton phase and more material is accreted. The same effect occurs when the rate of mass accretion is decreased because that lowers the rate of compressional energy production and, hence, slows the temperature rise. Implicit in these arguments is that, since the envelope is radiative, the time it takes radiation to reach the surface is an important parameter in determining the amount of time spent in the proton–proton phase of the TNR. As we have emphasized in this paper, increasing the opacity slows the rate of radiation transport, speeds the evolution time to the TNR, and reduces the amount of accreted material. In contrast, reducing the opacity lengthens the time to the peak and increases the amount of accreted material. Clearly, for a given WD luminosity and mass accretion rate, the way to lengthen the time spent in the proton–proton phase is to keep the opacity as small as possible.

The material being transferred by the donor star is assumed to have a solar mixture of elements and, thereby, a solar opacity. The assumption commonly made in calculations of accretion on to WDs is that this mixture is immediately enriched by core material (either by diffusion or shear mixing) which then increases the opacity and must, therefore, reduce the amount of accreted material in the given simulation. If one requires that the opacity be kept small, then these mechanisms either cannot be occurring or they cannot be mixing core material to the surface. These mechanisms, however, have been well studied both in nova simulations (Kovetz & Prialnik 1995; Iben et al. 1992a,b) and in other areas of astrophysics and we cannot assume, for some unknown reason, that they are not working in the case of accretion on to WDs.

To resolve this problem, therefore, we again refer to the analysis of the *ROSAT* observations of V1974 Cyg and GQ Mus which showed that there must be a layer of helium-rich material which remains on the surface of the WD after the outburst (Krautter et al. 1996; Starrfield et al. 1996a). We emphasize, in addition, that the large enrichments of helium in the ejecta of most novae (see Table 1) imply that a helium layer must be present on most of the WDs in nova systems. Although this layer will contain a significant fraction of heavy nuclei immediately after the end of an outburst, the long accretion times required to reach accreted masses of $5 \times 10^{-5}\,M_\odot$ or larger should provide sufficient time for these nuclei to gravitationally settle into the outer layers of the core. Given the existence of this helium layer, therefore, we claim that diffusion and shear mixing do occur but they do not mix accreted material into core material, they mix accreted material into the *remnant helium layer* on the WD.

One important consequence of mixing helium with the accreted material is that this also *reduces* the opacity in the surface layers (as long as the heavier nuclei have settled out of this layer) and will, therefore, lengthen the time to runaway and increase the amount of accreted material. A second and *more* important consequence of enriching helium is that this will have a major effect on the rate of nuclear energy production from the proton–proton reaction sequence. This is because the rate of the first reaction in the sequence, $^1{\rm H(p},\beta^+\nu)^2{\rm H}$, depends on X^2. Reducing the hydrogen mass fraction, therefore, will drastically reduce the rate of energy generation and slow the evolution to the peak of the TNR. We have verified the effects of an enriched helium layer on the time to TNR with new simulations to be described elsewhere (Starrfield et al., in preparation).

Nevertheless, given the existence and effects of the helium layer, we are still faced with the problem of enriching the accreted material with core material. We emphasize that the results from the abundance determinations (see sections 2 and 6) demand that core material be brought up into the accreted layers so that the mixture can be processed through hot, hydrogen burning and ejected into space.

Our proposed solution to the mixing problem is based on the existence and the properties of the convective region which first appears when the temperatures in the nuclear burning shell source exceed about 3×10^7 K. The convective region is a critical feature of the characteristics of the TNR since it regulates the temperature during the slow stages of the runaway and, subsequently, mixes core material to the surface. It also mixes surface material down to the nuclear burning region and keeps the nuclear reactions operating far out of equilibrium. Of importance to our solution is that multi-dimensional studies of this stage of evolution suggest that 'flames' develop and spread by small-scale turbulence (Fryxell & Woosley 1982; Shankar et al. 1992; Shankar & Arnett 1994).

Therefore, Glasner et al. (1997) and Kercek et al. (1997) have used two different two-dimensional, hydrodynamic codes to investigate the role of convection during the *peak* stages of the TNR. They both found that convection at the CEI entrains core material that is *below* the convective region (convective undershooting) and dredges it up into the accreted material, which can be enriched to more than 30 per cent. This is an important result since not only does it provide for a reasonable enrichment of the envelope, it indicates that this enrichment does not occur until the TNR is close to peak conditions and when the increased opacity, produced by the enriched nuclei, can no longer act to reduce the amount of accreted material. In addition, since the accreted gas has already been mixed with the helium layer by either diffusion or accretion-driven shear mixing, undershooting does not have to first penetrate some fraction of the helium layer before reaching core material. It is our claim, therefore, that all of the mechanisms proposed to mix accreted material with core material operate at some time during the accretion process.

Nevertheless, if it is undershooting at the peak of the TNR that is responsible for the envelope enrichment, then this has important and far-reaching implications for the current state of nova calculations. First, it allows us to accrete a mixture that consists of solar plus helium material (or possibly less than solar: Schwarz et al. 1997a), which results in a smaller opacity and a larger amount of accreted material.

Secondly, because it is the composition of the accreting material that determines the opacity, we expect differences in accretion times and nova characteristics for novae from different galactic populations (metallicity). If metallicity of the accreted material is important, for example, then we should expect differences between halo and disc novae as is observed (Della Valle et al. 1992). In addition, Large Magellanic Cloud (LMC) novae should be brighter and eject more material than Galactic novae of the same type since the LMC metallicity is about one-third that of the Galaxy. This is also observed (Della Valle et al. 1994). One caveat, however, is that previous outbursts should have polluted the secondary with high-Z ejecta which would then be transferred on to the primary reducing the metallicity effects. That this may not be taking place suggests that hydrodynamic studies of the interaction between the WD secondary and the expanding high-Z ejecta should be done.

Thirdly, we have identified two compositional classes of novae, those that occur on CO WDs and those that occur on ONeMg WDs (Starrfield et al. 1986). If ONeMg novae come from a younger population, so that the secondaries are transferring material with a higher metallicity, then we can expect differences in the characteristics of the explosions between these two classes in addition to the ejecta abundances.

Fourthly, if the WDs in these systems are rotating, then the amount of undershooting should vary on cylindrical shells and, unless there is a large amount of horizontal mixing at the peak of the outburst, there should be abundance differences from equator to poles. This could then manifest itself in observable abundance differences in the resolved nebulae. In addition, the latitudinal abundance differences should result in large differences in the rates of energy generation, peak temperature and energetics of the outburst from the equator to the poles. This variation, in turn, could be responsible for the non-spherical ejection observed in virtually all novae.

Fifthly, the amount of undershooting should depend on the composition of the accreting material and the mass, luminosity and rate of rotation of the WD. Therefore, the 'strength' of the outburst (usually attributed to the amount of core material mixed into the accreted layers) will depend, in some as yet undetermined way, on all these parameters. This implies the need for a new set of studies with large variations in these parameters plus the thickness of the helium shell.

Sixthly, the results of Glasner et al. (1997) and Kercek et al. (1997), in combination with the results reported in this paper, also have strong implications with respect to our understanding of the outbursts of recurrent novae (RNe). We note that both observations and theory imply that the RNe outbursts occur on massive WDs and require large mass accretion rates (Starrfield, Sparks & Truran 1985; Starrfield, Sparks & Shaviv 1988; Shore et al. 1991; Krautter et al. 1996). In addition, these same studies imply that only a small fraction of the accreted envelope is ejected and most of the material is burned to helium and remains as a thick layer on the WD. This is in contrast to what was found for V1974 Cyg where only a fraction of the accreted layers remained on the WD (Krautter et al. 1996). If the time-scales are too short for either accretion-driven shear mixing or diffusion to penetrate the helium layer, then it may also be the case that undershooting is unable to penetrate through the helium buffer layer and down into the core so that the ejected abundances will only be enriched in helium as is observed (Shore et al. 1991). This would imply that the large helium enrichment in RNe (cf. Shore et al. 1991) comes from the helium buffer material mixed up into the accreted envelope by undershooting.

Finally, if the accretion rate is low, then the outburst will occur above the CEI and, undershooting will not be able to mix down through the helium layer and dredge-up core material. This could explain why some slow novae, such as PW Vul (Saizar et al. 1991; Andreä et al. 1994; Schwarz et al. 1997b) eject material strongly enriched only in helium.

We emphasize that our explanation for the cause of too little mass being ejected in ONeMg nova outbursts is based on both recent observational and recent theoretical studies of these outbursts. The major differences between our proposed mechanism and the calculations that have been performed previously is the existence of a helium buffer layer between the newly accreted material and the core (implied by recent X-ray studies of novae by Krautter et al. 1996 and Shanley et al. 1995) plus the 2-dimensional calculations that indicate that mixing occurs by undershooting during the peak of the TNR (Glasner et al. 1997; Kercek et al. 1997).

8 SUMMARY AND DISCUSSION

In this paper we examined the consequences of the accretion of hydrogen rich material on to 1.25-$M_\odot$ ONeMg WDs in order to simulate the outburst of V1974 Cyg. We have, in particular, studied the effects of varying the convective efficiency ($\alpha = l/H_p$), the nuclear reaction rates, and the opacities on the characteristics of the simulations.

In order to investigate the effects of changes in α, we have

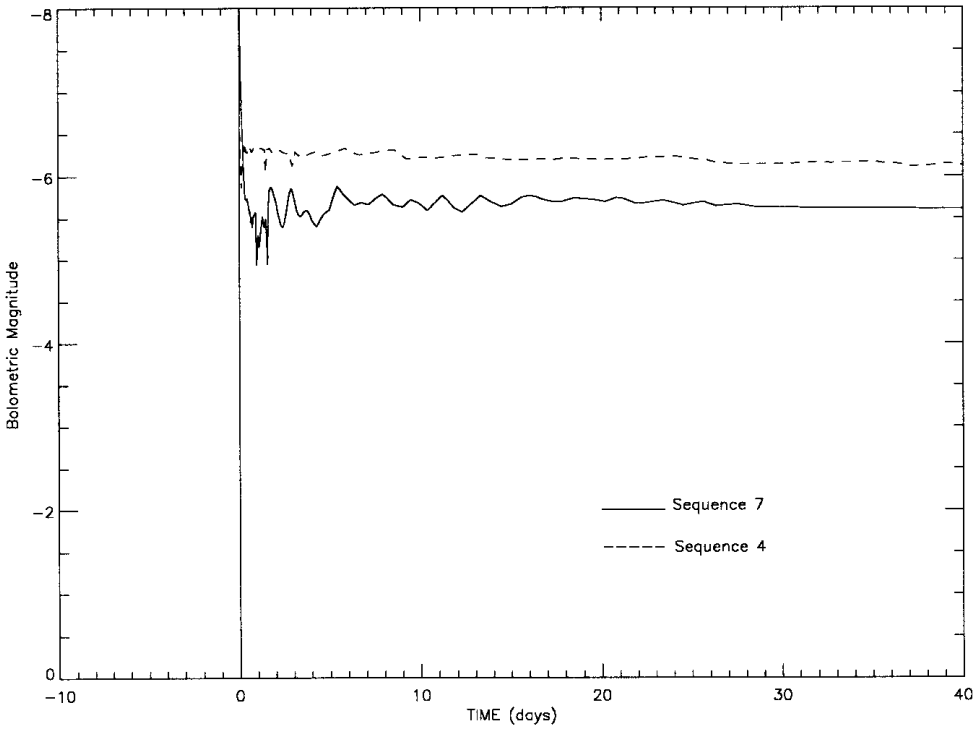

Figure 11. The absolute bolometric magnitude as a function of time for sequence 7 (solid line) and sequence 4 (dashed line) for the first 40 d (and 40 nights) after peak temperature occurs in the TNR. Note that, although peak luminosity is higher in sequence 7 than in sequence 4, the late time luminosity falls below sequence 4 because the opacity is higher in the envelope.

evolved two different sequences where the only change was to increase α by 1. In the first case, we increased α from 1 to 2 in order to demonstrate that the 1.25 $M_\odot$ evolutionary sequence presented in Politano et al. (1995), and computed with α=1, would eject more material at higher speeds if we used α=2. In the second case, we evolved sequences with α=2 (sequence 6) and α=3 (sequence 7), which were otherwise identical, in order to try to improve the agreement of our calculations with the observations of V1974 Cyg. In both cases, increasing the convective efficiency transported more heat and positron decay nuclei to the surface at the peak of the TNR. The increased energy deposition in the outer layers lifted them off the WD more rapidly which, in turn, ejected more material at higher speeds. It is clear, therefore, that the value of α used in simulating nova explosions can be an important parameter.

In a second comparison, we calculated a pair of nova simulations in which the only change was the nuclear reaction rate library (sequences 3 and 4). For sequence 3 we used the same rates as used in Politano et al. (1995) and in sequences 4, 5, 6, and 7 we used updated rates described in Van Wormer et al. (1994) and Herndl et al. (1995). This change had only marginal effects on the gross characteristics of the outburst but had major effects on the isotopic abundances for the intermediate mass nuclei. For example, the ejected abundance of ^{26}Al dropped from $\sim 10^{-2}$ to $\sim 10^{-3}$ and the abundance of ^{31}P jumped by over a factor of 2.

Our third and, as it turned out most important, change was to use the OPAL carbon-rich opacities in the outer layers. The OPAL opacities are larger than those obtained from the Iben fit to the Cox opacities at virtually all temperatures and densities. As was to be expected, the larger opacities made it easier to trap heat in the deeper parts of the accreted layers so that the TNR now occurred earlier with a smaller amount of accreted material (sequence 4O). Sequence 4O neither ejected sufficient material nor became sufficiently bright to resemble the outburst of V1974 Cyg. We then evolved a sequence where we reduced the central temperature of the WD to 10^7K. That sequence (sequence 5) accreted and ejected more material than sequence 4O but the amount of ejected mass was more than a factor of 10 smaller than what was observed for V1974 Cyg. In order to produce a simulation that actually ejected more material at higher speeds during the explosive stages of the outburst, we then reduced the mass accretion rate by a factor of 2. That sequence (sequence 6) ejected $\sim 5 \times 10^{-6}\,M_\odot$ at speeds exceeding 2000 km s^{-1}. Since these values were still lower than observed in the outburst of V1974 Cyg, we then evolved a simulation in which we increased α from 2 to 3. While this sequence (sequence 7) ejected more material at higher speeds than sequence 6, these parameters still did not agree with the observed values for the outburst of V1974 Cyg.

We emphasize, however, that the major disagreement is with the amount of ejected mass. Our abundance predictions (see Table 4) are in reasonable agreement with the observations of V1974 Cyg. In future calculations we will use improved values for the ONeMg initial abundances obtained from Ritossa et al. (1996) who have performed studies of the evolution of 10-$M_\odot$ stars through carbon burning. It is likely that by redoing our sequences with new abundances and comparing the predicted abundances with those observed we can, after a few iterations, determine the composition of the underlying WD.

The peak magnitudes of our theoretical light curves are also in reasonable agreement with the observations of V1974 Cyg. In Fig. 11 we show two light curves: one for sequence 7 (solid curve) and one for sequence 4 (dashed curve). Sequence 4 falls above sequence 7 because the opacity is lower and peak brightness increases as the

opacity decreases. Published values of the absolute bolometric magnitudes for V1974 Cyg range from −5.6 to −6.7 while our predicted bolometric magnitudes range around −6.

We also proposed a possible solution to the missing ejected mass problem based on the fact that for a given set of initial conditions (WD mass, luminosity, mass accretion rate) the total amount of mass accreted depends on the amount of time spent in the proton–proton burning phase of the evolution. The time spent in this phase depends on the rate of energy production by the proton–proton reaction sequence (which, in turn, depends on X^2) compared to the rate at which energy is transported to the surface and radiated. If the opacity is small, then the nuclear and compressional energy is rapidly transported to the surface and radiated, and the temperature grows slowly. A larger opacity traps more heat in the nuclear burning regions, the temperature rises more rapidly, and the time in the proton–proton phase decreases – for the same rate of mass accretion.

Previous studies carried out with either shear mixing or diffusion assume that the accreting layers are mixed with core material soon after accretion is initiated. This, in turn, enriches the low-Z (comparatively) material from the secondary star with high-Z core material, increases the opacity, and shortens the time to the TNR. The result is inescapable, core material cannot be mixed with accreted material during the accretion phase if the nova is to eject sufficient material to agree with the observations. Nevertheless, both of these mechanisms are probably operating during the accretion phase. We exit from this dilemma by noting that the *ROSAT* observations of V1974 Cyg and GQ Mus imply that a relatively thick layer of helium-rich material remains on the surface of the WD at the end of the outburst. Therefore, these two mechanisms must mix the accreted material with the helium-rich layer and not high-Z core material. This will decrease the opacity and lengthen the time to runaway.

The last problem that we discuss is how and when is the high-Z core material, observed in nova ejecta, actually dredged up into the accreted layers. We suggest that this mixing occurs near the peak of the TNR by undershooting (Woosley 1986) as found in the two-dimensional simulations of the TNR near peak temperature (Glasner et al. 1997; Kercek et al. 1997). If envelope enrichment occurs as a result of undershooting near the time of peak extent of the convective region, then during the accretion phase the abundances can be either solar or below solar. This would reduce the opacity from the values that we used in this study since we assumed that either shear mixing or diffusion was operating during the accretion phase. Nevertheless, we may need these two mechanisms to mix the accreted material with the helium layer early in the outburst because it is not clear that undershooting will be able to mix through the helium layer to core material. The mean molecular weight barrier might be too large.

Finally, we presented a number of implications of this mixing mechanism on the evolution and properties of the outburst. We are now investigating these new conditions in order to determine how much material can be accreted by the WD (Starrfield et al., in preparation). One important implication is that we can expect the characteristics of the outburst to depend on the metallicity of the material being transferred by the secondary star in the system. This result appears to be in agreement with the observations (Della Valle et al. 1992, 1994).

In summary we can say the following.

(i) Convective efficiency has a strong effect on the progress of the outburst. Increasing the convective efficiency, will increase the 'strength' of the outburst.

(ii) The opacity of the accreted material has a strong effect on the outburst since it determines the rate at which energy is transported away from the region where nuclear burning is occurring. Increasing the opacity, will reduce the amount of material accreted before the TNR.

(iii) Recent improvements in the nuclear reaction rates have not significantly changed the energetics of the outburst. They have, however, changed the nucleosynthesis predictions.

(iv) The observed ejecta abundances, in combination with the energetics, show that a significant fraction of the helium ejected during the outburst was produced in a prior outburst. The presence of this helium layer also influences the evolution to the peak of the TNR by reducing the hydrogen mass fraction and, thereby, the rate of energy generation by the proton–proton reaction sequence. Increasing the helium abundance, lengthens the time to TNR and increases the accreted envelope mass.

ACKNOWLEDGMENTS

We would like to thank M. Della Valle, R. D. Gehrz, A. Glasner, P. Hauschildt, M. Hernanz, W. Hillebrandt, I. Iben, J. Krautter, E. Livne, M. Politano, R. P. Kraft, H. Schatz, G. Schwarz, G. Shaviv, S. N. Shore, E. Sion, K. Vanlandingham, and R. M. Wagner for valuable discussions. This work was supported in part by NSF and NASA grants to the University of Chicago, to Notre Dame University, to Arizona State University, and by the DOE.

REFERENCES

Anders E., Grevesse N., 1989, Geochimica et Cosmochimica Acta, 53, 197
Andreä J., Drechsel H., Starrfield S., 1994, A&A, 291, 869
Arnett W. D., Truran J. W., 1969, ApJ, 157, 339
Austin S. J., Wagner R. M., Starrfield S., Shore S. N., Sonneborn G., Bertram R., 1996, AJ, 111, 869
Caughlan G., Fowler W. A., 1988, At.Dat.Nucl.Dat., 40, 291
Cox A. N., Stewart J. N., 1971, ApJS, 19, 243
Cox A. N., Tabor J. E., 1976, ApJS, 31, 271
Cox A. N., Kidman R., Starrfield S., Pesnell W. D., 1987, ApJ, 317, 303
Diehl R. et al., 1995, A&A, 298, 445
Della Valle M., Bianchini A., Livio M., Orio M., 1992, A&A, 266, 232
Della Valle M., Rosino L., Bianchini A., Livio M., 1994, A&A, 287, 403
Elliott J. R., 1996, MNRAS, 280, 1244
Ferland G. J., 1996, University of Kentucky Internal Report
Ferland G. J., Shields G. A., 1978, ApJ, 226, 172
Fowler W. A., Caughlan G. R., Zimmerman B. A., 1967, ARA&A, 5, 525
Fowler W. A., Caughlan G. R., Zimmerman B. A., 1975, ARA&A, 13, 69
Fryxell B., Woosley S. E., 1982, ApJ, 261, 332
Fujimoto M. Y., Iben I., 1992, ApJ, 399, 646
Gallagher J. S. et al. 1980, ApJ, 237, 55
Gehrz R. D., Grasdalen G. L., Hackwell J. A., 1985, ApJ, 298, L163
Gehrz R. D., Truvan J. W., Williams R. E., Starrfield S., 1998, PASP, 110, 3
Glasner S. A. Livne E., 1995, ApJ, 445, L149
Glasner S. A., Livne E., Truran J. W., 1997, ApJ, 475, 754
Görres J., Wiescher M., Rolfs C., 1989, ApJ 343, 356
Graff S., Görres J. Wiescher M., Azuma R. E., King J., Vise J., Hardie G., Wang T. R., 1990, Nucl. Phys., A510, 346
Harris M. J., Fowler W. A., Caughlan G. R., Zimmerman B. A., 1983, ARA&A, 21, 165
Hauschildt P. H., Wehrse R., Starrfield S., Shaviv G., 1992, ApJ, 393, 307
Hauschildt P. H., Starrfield S., Austin S. J., Wagner R. M., Shore S. N., Sonneborn G., 1994a, ApJ, 422, 831
Hauschildt P. H., Starrfield S., Shore S. N., Gonzalez-Riestra R., Sonneborn G., Allard F., 1994b, AJ, 108, 1008

Hauschildt P. H., Starrfield S., Shore S. N., Allard F. Baron E., 1995, ApJ, 447, 829
Hauschildt P. H., Baron E., Starrfield S., Allard F., 1996, ApJ, 462, 386
Hayward T. L. et al. 1996, ApJ, 469, 854
Herndl H., Görres J., Wiescher M., Brown B. A., Van Wormer L., 1995, Phys. Rev. C, 52, 1078
Hurlburt N. E., Toomre J., Massaguer J. M., Zahn J.-P., 1994, 421, 245
Iben I., 1992, in Warner B., ed., Variable Stars in Galaxies. Astron. Soc. Pac., San Francisco, p. 307
Iben I., Renzini A., 1983, ARA&A, 21, 271
Iben I., Fujimoto M. Y., MacDonald J., 1991, ApJ, 375, L27
Iben, I., Fujimoto M. Y., MacDonald J., 1992a, ApJ, 384, 580
Iben I., Fujimoto M. Y., MacDonald J., 1992b, ApJ, 388, 521
Iglesias C. A., Rogers F. J., 1993, ApJ, 412, 752
Iliadis C. et al. 1990, Nucl. Phys., A512, 509
Iliadis C. et al. 1991, Nucl. Phys., A533, 153
Iliadis C., Giesen U., Görres J., Wiescher M., Graff S. M., Azuma R. E., Barnes C. A., 1992a, Nucl. Phys., A539, 97
Iliadis C., Ross J. G., Görres J., Wiescher M., Graff S. M., Azuma R. E., 1992b, Phys. Rev., C45, 2989
Iliadis C., et al. 1993, Nucl. Phys., A559, 83
Iliadis C. et al. 1994, Nucl. Phys., A571, 132
Iliadis C., Buchmann L., Endt P. M., Herndl H., Wiescher M., 1996, Phys. Rev., C53, 475
Iliadis C. et al. 1997, Nucl.Phys. A, A621, 211
Kercek A., Hillebrandt W., Truran, J. W., 1997, A&A, submitted
Kovetz A., Prialnik D., 1985, ApJ, 291, 812
Kovetz A., Prialnik D., 1994, ApJ, 424, 319
Krautter J., Ögelman H., Starrfield S., Wichmann R., Pfefferman E., 1996, ApJ, 456, 788
Kutter G. S., Sparks W. M., 1987, ApJ, 321, 386
Kutter G. S., Sparks W. M., 1989, ApJ, 340, 985
Lance C. M., McCall M. L., Uomoto A. K., 1988, ApJS, 66, 151
Law W. Y., Ritter H., 1983, A&A, 63, 265
Livio M. 1994, in Shore S. N., Livio M., van den Heuvel E. P. J., eds Interacting Binaries: Sas Fee Advanced Course #22. Springer-Verlag, Heidelberg, p. 135
Livio M., Truran J. W., 1994, ApJ, 425, 797
MacDonald J., Fujimoto M. Y., Truran J. W., 1985, ApJ, 294, 263
Matheson T., Filippenko A., Ho C., 1993, ApJ, 418, L29
Metropolis N., Rosenbluth A., Rosenbluth M., Teller A., Teller E., 1953, J. Chem. Phys., 21, 1087
Morrisset C., Pèquignot D., 1996, A&A, 312, 135
Nofar I., Shaviv G., Starrfield S., 1991, ApJ, 369, 440
Nomoto K., Hashimoto M., 1988, Phys. Rep., 163, 13
Petitjean P., Boisson C., Pequignot D., 1990, A&A, 240, 433
Politano M., Starrfield S., Truran J. W., Sparks W. M., Weiss A., 1995, ApJ, 448, 807
Prialnik D., Kovetz A., 1984, ApJ, 281, 367
Prialnik D., Kovetz A., 1995, ApJ, 445, 789
Press W. H., Teukolsky S. A., Vetterling W. T., Flannery B. P., 1992, Numerical Recipes. University Press, Cambridge
Ritossa C., Garcia-Berro E., Iben I., 1996, ApJ, 460, 489
Ritter H., Politano M., Livio M., Webbink R., 1991, ApJ, 376, 177
Rogers F. J., Swenson F. J., Iglesias C. A., 1996, ApJ, 456, 902
Ross J. G. et al. Phys.Rev., C52, 1681
Saizar P., Ferland G. J., 1994, ApJ, 425, 755
Saizar P. et al., 1991, ApJ, 367, 310
Saizar P. et al., 1992, ApJ, 398, 651
Saizar P., Pachoulakis I., Shore S. N., Starrfield S., Williams R. E., Rotschild E., 1996, MNRAS, 279, 280
Schmidt S. et al., 1995, Nucl.Phys., A591, 227
Schwarz G. J., Hauschildt P. H., Starrfield S., Baron E., Allard F., Shore S. N., Sonneborn G., 1997a, MNRAS, 284, 669
Schwarz G. J., Starrfield S., Shore S. N., Hauschildt P. H., 1997b, MNRAS, 290, 75
Seuthe S. et al., 1990, Nucl.Phys. A514, 471
Shankar A., Arnett D., 1994, ApJ, 433, 216
Shankar A., Arnett D., Fryxell B. A., 1992, ApJ, 394, L13
Shanley L., Ögelman H., Gallagher J., Orio M., Krautter J., 1995, ApJ, 438, L95
Shore S. N., Sonneborn G., Starrfield S., Hamuy M., Williams R. E., Cassatella A., Drechsel, H., 1991, ApJ, 370, 193
Shore S. N., Sonneborn G., Starrfield S., Gonzalez-Riestra R., Ake, T. B., 1993. AJ, 106, 2408
Shore S. N., Sonneborn G., Starrfield S., Gonzalez-Riestra R., Polidan R., 1994, ApJ, 421, 344
Shore S. N., Starrfield S., Sonneborn G., Gonzalez-Reistra R., 1996, ApJ, 463, L21
Shore S. N., Starrfield S., Ake T. B., Hauschildt P. H., 1997, ApJ, 490, 393
Snijders M. A. J., Batt T.J., Roche P. F., Seaton M. J., Morton D. C., Spoelstra T. A. T., Blades J. C., 1987, MNRAS, 228, 329
Sparks W. M., Kutter G. S., 1987, ApJ, 321, 394
Sparks W. M., Starrfield S., Truran J. W., Kutter G. S., 1988, in Nomoto K., ed., Proc. IAU Colloq. No. 108, Atmospheric Diagnostics of Stellar Evolution: Chemical Peculiarity, Mass Loss, and Explosion. Springer-Verlag, Berlin, p. 234
Sparks W. M., Kutter G. S., Starrfield S., Truran J. W., 1990, in Cassatella A., Viotti R., eds, Physics of Classical Novae. Springer-Verlag, Heidelberg, p. 361
Starrfield S., 1988, Cordova F. A., ed., in Multiwavelength Observations in Astrophysics. University Press, Cambridge, p. 159
Starrfield S., 1989, in Bode M., Evans A., eds, The Classical Novae. Wiley, New York, p. 39
Starrfield S. 1993, in Sahade J., McCluskey G. E., Kondo Y., eds, The Realm of Interacting Binary Stars. Kluwer, Dordrecht, p. 209
Starrfield S. 1995, in Roxburgh I., Masnou J. L., eds, Physical Processes in Astrophysics. Springer, Heidelberg, p. 99
Starrfield S., Truran J. W., Sparks W. M., 1978, ApJ, 226, 186
Starrfield S., Sparks W. M., Truran J. W., 1985, ApJ, 291, 136
Starrfield S., Sparks W. M., Shaviv G., 1988, ApJL, 326, L35
Starrfield S., Sparks W. M., Truran J. W., 1986, ApJ, 303, L5
Starrfield S., Shore S. N., Sparks W. M., Sonneborn G., Politano M., Truran J. W., 1992a, ApJ, 391, L71
Starrfield S., Politano M., Truran J. W., Sparks W. M. 1992b, in Schrader C., Gehrels N., Dennis B., eds, Second GRO Science Conference. NASA: CP 3137, 377
Starrfield S., Truran J. W., Politano M., Sparks W. M., Nofar I., Shaviv G., 1993, Physics Reports, 227, 223
Starrfield S., Krautter J., Shore S. N., Idan I., Shaviv G., Sonneborn G. 1996, in Bowyers S., Malina R., eds, Astrophysics in the Extreme Ultraviolet. Kluwer, Dordrecht, p. 419
Stegmüller F., Rolfs C., Schmidt S., Schulte W. H., Trautvetter H. P., Kavanagh R. W., 1996, Nucl.Phys. A, 601, 168
Stickland D. J. et al. 1981, MNRAS, 197, 107
Timmermann R., Becker H. W., Rolfs C., Schröder U., Trautvetter H. P., 1989, Nucl. Phys., A477, 105
Truran J. W., 1982, in Barnes C. A., Clayton D. D., Schramm D. N., eds, Essays in Nuclear Physics. University Press, Cambridge, p. 467
Truran J. W., 1990, in Cassatella A., Viotti R., eds, The Physics of Classical Novae. Springer, Heidelberg, p. 373
Truran J. W., Glasner A., 1995, in Bianchini A., Della Valle M., Orio M., eds, Cataclysmic Variables. Kluwer Academic, Dordrecht, p. 453
Truran J. W., Livio M., 1986, ApJ, 308, 721
Tylenda R., 1978, Acta Astronomica, 28, 333
Vanlandingham K., Starrfield S., Wagner R. M., Shore S. N., Sonneborn G., 1996, MNRAS, 282, 563
Vanlandingham K., Starrfield S., Shore S. N., 1997, MNRAS, 290, 87
Van Wormer L., Görres J., Iliadis C., Wiescher M., Thielemann F. K., 1994, ApJ, 432, 326
Wallace R. K., Woosley S. E., 1981, ApJ, 45, 389
Weiss A., Truran J. W., 1990, A&A, 238, 178
Williams R. E., Gallagher J. S., 1979, ApJ, 228, 482
Williams R. E., 1978, ApJ, 224, 171

Williams R. E., Ney E. P., Sparks W. M., Starrfield, S., Truran J. W., 1985, MNRAS, 212, 753
Woodward C. E., Gehrz R. D., Jones T. J., Lawrence G. F., 1992, ApJ, 384, L41
Woodward C. E., Gehrz R. D., Jones T. J., Lawrence G. F., Skrutskie M. F., 1997, ApJ, 477, 817
Woosley S. E. 1986, in Houck B., Maeder A., Meynet G., eds, Nucleosynthesis and Chemical Evolution: Sas Fee #16. Geneva Observatory, Sauverny, p. 1
Woosley S. E., Fowler W. A., Holmes J. A., Zimmermann B. A., 1975, Caltech preprint OAP-422

This paper has been typeset from a $\TeX$/$\LaTeX$ file prepared by the author.